Prospero Joseph, M. (Orcid ID: 0000-0003-3608-6160)
Barkley Anne (Orcid ID: 0000-0001-5260-2538)
Gaston Cassandra, J. (Orcid ID: 0000-0003-1383-8585)

Characterizing and quantifying African dust transport and deposition to South America: Implications for the phosphorus budget in the Amazon Basin

Joseph M. Prospero[1*], Anne E. Barkley[1], Cassandra J. Gaston[1], Alexandre Gatineau[2], Arthur Campos y Sansano[2]; Kathy Panechou[2]

[1]Rosenstiel School of Marine and Atmospheric Sciences, University of Miami, Miami, FL, 33149, USA; [2] ATMO Guyane, Remire-Montjoly, 97343 Guyane (French Guiana), France.

*Joseph M. Prospero (jprospero@miami.edu)

Key Points:

- We use fifteen years of aerosol measurements in trade winds at Cayenne, French Guiana, to quantify the transport of African dust to South America in boreal Spring.
- Dust transport may be supplying significant amounts of nutrients, including phosphorus, that are important for maintaining soil fertility in the Amazon Basin.
- The MERRA-2 model yields deposition rates to the Amazon that are significant but substantially smaller than rates from previous studies.

Accepted Article

This article has been accepted for publication and undergone full peer review but has not been through the copyediting, typesetting, pagination and proofreading process which may lead to differences between this version and the Version of Record. Please cite this article as doi: 10.1029/2020GB006536

©2020 American Geophysical Union. All rights reserved.

Abstract

Soils in the Amazon Basin are deficient in phosphorus, essential to soil fertility. Previous studies suggested that African mineral dust deposited to Amazonian soils served as an important source of phosphorus that enhances soil fertility. These studies lacked the quantitative measurements essential to validate estimates. Here we present daily measurements of mineral dust and PM_{10} carried in the Trade Winds at Cayenne, French Guiana, during 2002 - 2017. MERRA-2 model dust concentrations showed excellent agreement with measurements over this period. Consequently, we used MERRA-2 to estimate temporal and spatial deposition rates to Amazonia. Our annual deposition rate, 8 – 10 Tg dust, is substantially lower than previous estimates. Deposition rates are greatest over the northern and north-eastern regions of South America. In contrast, rates are low in central Amazonia. Our results raise questions about the impact of African dust on soil fertility in Amazonia. However, African aerosol transport carries other aerosol species that could play a role in soil fertility, including biomass burning products known to contain substantial concentrations of phosphorus. Our study highlights the need for more measurements of aerosol and precipitation chemistry over wider expanses of South America in order to better characterize aerosol chemical and physical properties, to identify aerosol sources, and to constrain model estimates. We show that over 2002 – 2017 dust transport to South America was negatively correlated to rainfall over the Sahel in North Africa. Long-term monitoring is needed to capture changes in transport from Africa that might occur as a result of climate change.

Plain Language Summary

The Amazon Basin plays a major role in climate by removing huge quantities of carbon dioxide (CO_2) from the atmosphere and storing the carbon in vegetation. This removal partially offsets the impact of CO_2 emitted by humans and the consequent rate of global warming. There is a concern about decreasing soil fertility in the Amazon Basin because of the loss of phosphorus, an essential plant nutrient, due to intense tropical weathering and biomass burning. Previous work suggested that large quantities of dust are transported from Africa to South America every year and deposited to the Amazon. Dust contains phosphorus and other nutrients that could mitigate soil losses and increase Amazonian soil fertility. However, estimates of the amount of dust carried to the Amazon are uncertain because of the lack of aerosol measurements. Our multi-year measurements of African dust in the Trade Winds in French Guiana data, coupled with a chemical transport model, suggest that significant quantities of dust reach the heart of the Amazon Basin although substantially less than had been previously estimated. This raises questions about the long-term status of soil fertility in the Amazon and the future impact on the carbon cycle. We also find that the quantities of dust transported to South America are inversely linked to rainfall in North Africa. Consequently, climate change will affect dust transport to South America.

.

Accepted Article

©2020 American Geophysical Union. All rights reserved.

1 Introduction

Forests play an important role in climate by taking in large quantities of atmospheric CO_2 and sequestering the carbon in biomass. Tropical forests are of particular importance because they account for about half the global forest carbon budget (Pan et al., 2011). In this context, the Amazon Basin is of great interest because it is one of the largest ecosystems on Earth. There is concern about changes that might occur in the Amazon due to deforestation, biomass burning (BB) (Artaxo et al., 2013) and the loss of soil fertility (Brienen et al., 2015), processes that might ultimately impact the global carbon cycle.

As is the case with many tropical forests (Mercado et al., 2011), the ecosystem in the Amazon is phosphorus (P) limited rather than nitrogen limited. The soils in the Amazon are depleted in various elements because of intense weathering in the hot, humid environment and because of losses due to widespread BB (Das et al., 2011; Mahowald et al., 2005; Okin et al., 2004). Smoke rich in P and other nutrients is carried out of the region by winds (Mahowald et al., 2005; Myriokefalitakis et al., 2016) leading to a net loss of P and base metals (Boy & Wilcke, 2008; Mahowald et al., 2005; Tipping et al., 2014).

There is an increased interest in the role that African dust might play as a source of nutrients for Amazonian soils. This interest evolved over the years beginning with the studies on Barbados in the mid-1960s that showed that large quantities of African dust are carried into the western North Atlantic and Caribbean during boreal summer (Delany et al., 1967; Prospero, 1968; Prospero et al., 1970; Prospero & Nees, 1977). Building on this research, in 1978 Prospero et al., (1981) initiated an aerosol sampling program in Cayenne, French Guiana (FG), 04.948°N, 52.309°W (Figure 1) with the expectation that large quantities of African dust might also be carried in the latitudes south of Barbados in concert with the seasonal southward shift of the large scale wind system over the Atlantic, a process that would later be substantiated by many satellite aerosol products (e.g., Adams et al., 2012; Chin et al., 2014; Hsu et al., 2012; Mehta et al., 2016; Shikwambana & Sivakumar, 2018; Yu et al., 2015a,b).

Daily sampling at Cayenne over 1978 – 1979 (Prospero et al., 1981) showed that African dust transport in boreal winter and spring was equal to that measured at Barbados in summer. Their study served to stimulate a broader interest in dust transport to South America (henceforth, SA) beginning with Swap (Swap et al., 1992) who reported on measurements at a site in the Amazon Basin near Manaus, Brazil (see Fig. 1, ATTO) that showed the prominent presence of mineral dust. Based in part on the work of Prospero et al., Swap et al. attributed this dust to African sources and speculated that dust could play an important role in supplying nutrients including P to the Amazon basin.

The Swap *et al.* study led to a series of programs that touched on the transport issue. (See Martin et al., (2010) and Andreae et al., (2015) for reviews of aerosol field programs in the region.) Building on this work, recent efforts (see Yu et al., 2015a; Yu et al., 2015b) have attempted to link dust transport to Amazon deposition. These assessments were based largely on satellite and modeling studies and on occasional field campaigns and sporadic measurements in the Amazon Basin. These studies established that African dust was indeed carried into the interior of the Amazon Basin, but they did not provide a sense of the quantitative impact on the Basin at large or the temporal-spatial variability.

Despite this interest, no further long-term aerosol measurements were made in the region that could serve as the basis for an assessment until the early 2000s when air quality

©2020 American Geophysical Union. All rights reserved.

measurements began in FG. These included the measurement of PM_{10}, particles less than 10 µm diameter. Prospero et al., (2014) compared PM_{10} data from FG, Guadeloupe and Martinique to dust measurements on Barbados (Prospero & Lamb, 2003; Prospero & Mayol-Bracero, 2013) to show that elevated PM_{10} concentrations could reasonably be attributed to the advection of African dust and that, consequently, PM_{10} could be used as a proxy for dust. Nevertheless, it was not possible to quantitatively link measurements of PM_{10} to actual measurements of mineral dust at those sites.

In this work, we attempt to better characterize and quantify the transport and deposition of African dust to SA with a focus on the Amazon Basin. Our study is based on 10 months of daily mineral dust samples collected with filters exposed in the Trade Winds at a coastal site at Cayenne. We compare these data with concurrently-made PM_{10} measurements carried out as a component of the French national air quality program in Cayenne, and we quantitatively show that PM_{10} concentrations greater than about 15-20 µg m^{-3} can be almost entirely attributed to advected mineral dust as previously suggested (Prospero et al., 2014). We next compare our monthly-averaged Cayenne PM_{10}-dust record to the surface dust model product from MERRA-2 (Modern-Era Retrospective Analysis for Research and Applications, version 2; Gelaro et al., 2017; Randles et al., 2017) and we show excellent agreement. We then use MERRA-2 to estimate dust transport and deposition to SA north of 10°S, and we show how they vary temporally and spatially. We close with a discussion of measurement strategies that are needed to properly quantify aerosol budgets and elucidate aerosol cycles over SA.

2 Materials and Methods

2.1. PM_{10}

As a Department of France, FG is subject to the same national air quality standards and it is required to monitor ambient conditions following the same protocol as that carried out in mainland France. Measurements are performed under the direction of ATMO-Guyane, a non-profit organization, approved by the ministry in charge of environmental oversight for monitoring air quality in FG [https://www.atmo-guyane.org/]. All data were obtained using TEOM (tapered element oscillating microbalances) instruments [ThermoFischer Scientific] which measure in near-real-time the atmospheric mass concentration of aerosol particles less than 10 um diameter. (See Text S1)

2.2. Hi-Vol Filter Sampling:

In 2014, a high-volume aerosol sampling system was installed at a site situated in a protected area on the top of a 67 m wooded hill (4.949°N, 52.310°W) located directly on the northeast coast of the city of Cayenne, population 57,000 (see Figure S1). Cayenne lies in the Trade Wind belt. Winds have a strong northeasterly component in boreal winter. Winds shift more easterly-southeasterly in summer (see Figure S2 for monthly wind roses.) This shift reflects changes in large scale wind fields as shown in HYSPLIT back trajectories (Figure S3). Sampling is carried out by personnel of ATMO. Filters are changed on a nominal 24-hour cycle starting around local noon. Samples are collected on Whatman 41 filters which are periodically returned to Miami for analysis. The filters are extracted with water to remove soluble species which are primarily comprised of sea-salt. The filters are then reduced to ash in a furnace. The residue is ascribed to mineral dust. Elemental analyses of African dust (Arimoto et al., 1995; Bozlaker et al., 2017, 2019; Trapp et al., 2010) yield concentrations of major (and many minor) elements close to those of average crustal materials (Rudnick & Gao, 2003). See Text S1 for a detailed description of the sampling and analysis protocol.

©2020 American Geophysical Union. All rights reserved.

2.3 MERRA-2 Model and Products

The Modern-Era Retrospective analysis for Research and Applications, version 2 (MERRA-2) is a global atmospheric reanalysis product of the NASA Global Modeling and Assimilation Office (GMAO) (Gelaro et al., 2017). MERRA-2 generates a regularly-gridded, homogeneous record of the global atmosphere that includes various aspects of the climate system including aerosols. MERRA-2 is based on the Goddard Earth Observing System, version 5 (GEOS-5) atmospheric model and has a spatial resolution 0.5° latitude by 0.66° longitude and, in the vertical, 72 layers (Randles et al., 2017). MERRA-2 uses the interactive Goddard chemistry, aerosol, radiation, and transport (GOCART) model (Chin et al., 2002; Colarco et al., 2010) to simulate the sources, sinks, and chemistry of five externally mixed aerosol species: mineral dust, sea salt, black carbon, organic carbon, and sulfate. MERRA-2 is unique among models in that it assimilates satellite-made observations of aerosols and represents their interactions with other physical processes. Since 2000, MERRA-2 largely uses the Moderate Resolution Imaging Spectroradiometer (MODIS) (Randles, 2016; Randles et al., 2017). With the assimilation of MODIS data, we might expect that MERRA-2 would yield improved representations of global aerosol distributions and deposition compared to other models. The MERRA-2 product has been extensively tested against measurements of a wide range of aerosol types including mineral dust measurements made at the University of Miami research site at Barbados (Fig. 1) and found to produce excellent results (Randles et al., 2016, 2017; Buchard et al., 2017). Comparisons of MERRA-2 aerosol products with *in situ* measurements of PM at sites in the United States have shown that the model provides consistently accurate estimates during African and Asian dust events (Chen et al., 2018). Similarly, comparisons of MERRA-2 aerosol vertical distributions compare well with CALIOP vertical distributions (Chen et al., 2018).

In this study, we use the MERRA products available on the NASA GIOVANNI web site (http://disc.sci.gsfc.nasa.gov/giovanni) where a variety of dust products are available including surface mass concentration (DUSMASS) and column-integrated values (DUCMASS). Also available is a range of wet and dry deposition products. We use the total dust dry-plus-wet deposition product (DUDPWTSUM). At Cayenne, according to MERRA-2, wet deposition is by far the most important mechanism.

3 Results

3.1. Relating Cayenne PM_{10} Air Quality Measurements to Mineral Dust Concentrations.

In 2014, PM_{10} measurements were made at four stations in FG although all stations were not necessarily in operation at all times. Figure 2 shows the daily PM_{10} averaged for all stations. The PM_{10} daily means at individual sites in the years 2014 through 2017 are shown in Fig. S4. The records at the various sites closely track one another and demonstrate in detail the consistency of the seasonal pattern of PM_{10}. The close agreement among the sites during dust episodes is evidence that local and regional sources do not account for large spikes in PM_{10} concentration. It is notable that one station, Kourou, is located on the coast 60 km northwest of the Cayenne metropolitan area and yet the record at that site is synchronous with the Cayenne sites. Also shown in Fig. 2 are the dust concentrations measured from the filter analyses.

Early in the year through June, daily PM_{10} concentrations in Fig. 2 broadly track the measured filter-based dust concentrations. In 2014, there were long periods in February through May when substantial amounts of dust were present, with notably large peaks: 181 μg m^{-3} PM_{10} on 04 March and 134 μg m^{-3} PM_{10} on 05 March. This event is directly linked to

©2020 American Geophysical Union. All rights reserved.

a major dust outbreak along the west coast of North Africa on 28 February as shown in MODIS images, Fig. S5. This outbreak could be followed across the Atlantic in MODIS AOD daily sequences (https://worldview.earthdata.nasa.gov/). Fig. S5 shows the AOD distribution off the coast of Africa on 28 February and on 03 March when the plume begins to encroach on the coast of FG. The transit time of 5 days is typical of such events.

The record in Fig. 2 is consistent with our expectations based on similar filter-based dust measurements made in Cayenne in the late 1970s (Prospero et al., 1981) and a recent study of Cayenne PM_{10} (Prospero *et al.*, 2014). The dust season begins in December and ends abruptly in June as evidenced by a distinct change in the character of the PM_{10} record. Starting in July, values fall in a relatively narrow band between about 18 – 25 μg m^{-3} while filter-based dust concentrations dropped to very low levels, only a few micrograms per cubic meter. In 2014, there were four PM_{10} systems in operation in Cayenne although all four did not consistently come on-line until later in the year (Fig. S4a). It is noteworthy that the period of low aerosol concentration extends through the dry season, August through November (minimum rainfall in September and October, 30 – 40 mm) when one might expect local dust sources, if any, to be most active. This same pattern is also seen in 2015, 2016 and 2017 (see Fig. S4b,c,d).

The character of the PM_{10} record changes markedly in October 2014 when concentrations drop sharply in a coherent way to lower values in the range of about 10 – 20 μg m^{-3} (Fig. 2). The marked change in the character in these two months is also clearly seen in Fig. S4 in the records for 2015 and 2017 – but not in 2016. Nonetheless, the July-November record provides a reference base with which to scale the impacts we might expect to see from local sources which we expect to be primarily sea-salt aerosol.

Continuing through the record in Fig. 2, on 17 December 2014, PM_{10} increases sharply, evidence of the beginning of the next dust season that will extend into 2015 (see the continuation in Fig.S4b). In some years, the onset of the dust season can be quite dramatic, e.g., December 2015 and 2017, S4b,d. In contrast, in 2016 (S4c) the onset of the following year dust season is unusually late. Similarly, the end of the dust season can be quite abrupt as seen in 2015 and 2017.

As noted above in Fig. 2, filter dust concentrations track those of PM_{10} in a general way. But it is difficult to make a close comparison for two reasons. First, as noted above, the start time for the filter samples was not synchronized with the PM_{10} measurements. Because many dust events occur as sharp spikes, the average over the filter sampling period could differ substantially from that measured as PM_{10}. Second, many filters (47 out of a total of 148) were collected over a period of two or more days which will tend to level out peaks and valleys in the concentration record.

In Fig. 2, the left inset shows a scatter plot of PM_{10} against average dust based on all filter measurements; the right inset shows only data from multi-day filters. The latter yields an improved scatter plot because the averaging minimizes the impact of the time differential between the PM_{10} measurement cycle and that of the filter protocol. In the range of the low dust concentration values (i.e., below about 10 μg m^{-3}), PM_{10} values cluster between about 17 – 22 μg m^{-3}, a range that can be regarded as the operational regional background. We expect the background to be largely due to sea salt aerosol based on our work at Barbados where monthly mean sea-salt concentrations range from 14.6 to 21.6 μg m^{-3} (Savoie et al., 1989, 2002). Thus, PM_{10} values above this range can serve as a proxy for advected dust. Studies in South Florida (Prospero et al., 2001) and in an aircraft program in Surinam (Formenti et al.,

©2020 American Geophysical Union. All rights reserved.

2001) show that African dust mass falls almost entirely in the size range under 10 μm diameter.

3.2. Large Scale Setting of Cayenne Dust Events

The presence of dust at this time of year is consistent with the picture provided by various satellite products, in particular, the spaceborne lidar CALIOP (Cloud-Aerosol Lidar with Orthogonal Polarization aboard the satellite CALIPSO (Cloud-Aerosol Lidar and Infrared Pathfinder Satellite Observations, Winker *et al*., 2010). CALIOP yields aerosol vertical distributions and a qualitative speciation of the aerosol mass (Adams et al., 2012). Tsamalis et al., 2013) use CALIOP in a detailed study of Saharan dust transport across the Atlantic and Yu et al., (2015a) use CALIOP to assess transport across the Atlantic and deposition to the Amazon Basin Yu et al., 2015b).

Many of the large dust events documented in Fig. 2 could be linked to prominent dust layers seen in CALIOP when the track passes within a few degrees of Cayenne. Figure 3 shows an example on 30 April 2014 during an extended period (from mid-April through the first week of May when PM_{10} concentrations were consistently in the range of 40 to 60 μg m^{-3}. Over Cayenne, CALIOP shows a deep layer that extends to an altitude of about 3.0 to 3.2 km. The same track passed east of Barbados and shows the layer extending north to about 22°N – 23°N. CALIOP also shows dust extending south to about 3°N where it becomes lost in cloud and rain in the ITCZ. Thus, this event yielded a total latitude spread of about 20 degrees. A cursory examination of all CALIOP tracks that passed close to Cayenne during January through May 2014 yielded a total of 21 days when our measurements of dust at the surface coincided with the advection of deep layers of African dust.

The dust event on 30 April at Cayenne (Fig. 2) also yields the typical meteorological signature of the Saharan Air Layer (SAL), which is often seen in the presence of dust outbreaks during boreal summer over the Atlantic and Caribbean (Carlson, 2016; Carlson & Prospero, 1972). The presence of the SAL is identified in meteorological sondes as an elevated layer of hot dry air. A segment of the sonde profile often shows a layer with a constant potential temperature of about 40°C and mixing ratios of only a few grams per kilogram, properties that were initially established in deep mixing layers over the Sahara (Carlson, 2016; Karyampudi et al., 1999). The Barbados profile shows the classical features of the SAL.

The greatest dust concentrations are typically found within the SAL as shown by aircraft measurements of aerosol physical and chemical properties and lidar profiles over the Caribbean (Groß et al., 2015; Prospero & Carlson, 1972; Weinzierl et al., 2017) although dust obviously extends down to the surface as seen in CALIOP. On 30 April, the SAL over Cayenne is much more shallow than at Barbados although the SAL layer has the same potential temperature and mixing ratio at both sites. In general, the altitude of the top of the SAL at Cayenne in the main dust season, December to April, is about 2 – 3 km (Huang, Zhang, et al., 2010; Tsamalis et al., 2013) while at Barbados in its dust season, JJA, it is at about 4 – 5 km (Ben-Ami et al., 2009; Huang, Zhang, et al., 2010; Rittmeister et al., 2017; Tsamalis et al., 2013; Weinzierl et al., 2017).

However, on most days during dust events at Cayenne, the SAL signature is less obvious than in this example. The SAL is particularly well-defined here because of the size and intensity of the event which can be linked to the emergence of dense clouds of dust off the coast of Africa beginning in late April (Fig. S5). These outbreaks yielded very large MODIS aerosol optical

©2020 American Geophysical Union. All rights reserved.

depth (AOD) values over a huge area of the tropical and equatorial Atlantic (Fig. S6). Under more typical conditions in winter and spring, because of the proximity of the dust transport paths to the ITCZ in the latitude of Cayenne, the dust events are often affected by rain that will remove dust. Indeed, in the sonde profile at Cayenne in Fig. 3, the atmosphere from the surface to the base of the SAL at 2 km is saturated suggesting that it had been raining, which is typical during the rainy season.

While CALIOP can be used to track dust events over the Amazon Basin, the presence of persistent heavy cloud and rain and the presence of BB aerosol can complicate dust detection with CALIOP (Tsamalis et al., 2013). Nonetheless, over the Amazon, ground-based lidars (e.g., at ATTO, Fig. 1) frequently show elevated layers that can often be linked to dust (and smoke) transported from Africa (Ansmann et al., 2009; Baars et al., 2011).

The seasonal cycle of dust transport to Cayenne, and to SA in general, is closely linked to the seasonal progression of the ITCZ and the associated changes in the large-scale circulation over the Atlantic. The relationship between dust transport to this region and movement of the ITCZ and the SAL is characterized in detail by (Tsamalis et al., 2013). In the longitude of Cayenne, the ITCZ is observed between 5°S and 10°N in winter and 10°N to 15°N in summer. The migration of the ITCZ over land is somewhat different from that over the ocean (Bovolo et al., 2012). The seasonal movement of the ITCZ is generally greater over land. It moves north during May–July to a position approximately 7°N (i.e., over Cayenne) and southwards during November–January to a position around 15°S, placing it over the southern Amazon Basin. Accordingly, during the dust season at Cayenne, transport will be strongly modulated by the meandering of the ITCZ. In boreal summer, Cayenne lies to the south of the ITCZ which serves to cut off dust transport from North Africa. The dramatic change in aerosol character from May-June to December is consistent with what we would expect from the movement of the ITCZ. Nonetheless, occasional dust events manage to penetrate deep into the ITCZ (Huang et al., 2010).

3.3. The Cayenne PM_{10} Record: 2002 – 2017.

Our dust measurements during 2014 show excellent agreement with PM_{10}. (Barkley et al., 2019) report on a similar dust study at Cayenne in 2016 using the same equipment and protocols and they report similar results. On this basis, we examine the entire Cayenne PM_{10} record to characterize the interannual variability and the implications for dust transport. Figure 4 shows the daily mean TEOM PM_{10} concentrations from Cayenne, 2002 to 2017. There is a clear seasonal periodicity that is consistent with that observed in 2014 although there is considerable inter-annual variability.

To present a climatological picture of transport, in Fig. 4 right, PM_{10} concentrations are plotted against the day-of-the-year. This abrupt end of the dust season in late May is linked to the migration of the ITCZ and a shift to southeasterly winds as seen in wind roses (Fig. S2) and in HYSPLIT back trajectories (Fig. S3). As shown in (Barkley et al., 2019), aerosols arriving at Cayenne from about day 140 to around day 340 have their origins primarily in southern Africa where there are few large dust sources (Prospero et al., 2002). This change is also clearly discernible in the change of the filter colors (see Barkley et al., (2019), their Fig. S5 and S8) which have a beige tinge during the dust season and, in contrast, a distinct gray coloration between May and December which suggests the dominant presence of BB products. Even during the dust season, there is a clearly visible gray undertone to the beige dust coloration which suggests the presence of substantial BB aerosol, typically transported from sources in southwest West Africa and coastal states on the Gulf of Guinea.

©2020 American Geophysical Union. All rights reserved.

The year-to-year consistency of the broad peak in September-October is remarkable and suggests that it is controlled by seasonal changes in sources and transport patterns. The sharpness of the transition after day 280 stands out more clearly in the time series in Fig. 4, left, where in many years the transition appears as a sharp peak in daily PM_{10} values.

3.4. PM_{10}-Dust and MERRA-2

In section *3.1,* the comparison of the filter-based dust measurements with PM_{10} suggests that $PM_{10,}$ when adjusted for background, can serve as a reliable proxy for advected African dust. In Figure 5, we plot the monthly means of the daily average PM_{10} data from Cayenne over the period 2002 – 2017 after subtracting the "background" value of 16.9 μg m^{-3}, the Y-intercept in Fig. 2, inset. We henceforth refer to these adjusted values as "PM_{10}-Dust". In Fig. 5, we also plot the monthly mean surface dust concentrations obtained from MERRA-2, extracted in a one-degree by one-degree box centered on Cayenne. In Fig. 5, MERRA-2 estimates of surface dust concentrations track the PM_{10}-Dust concentrations very well during the nominal dust season. Indeed, in 2014, the MERRA-2 dust peak overlaps the PM_{10}-Dust peak almost perfectly except for June.

Over 2002 – 2017, the model correctly identified the peak month in almost every year although MERRA-2 tended to slightly overestimate the concentration in the peak month, especially early in the record. The model also did well in capturing the inter-annual variability, in particular, the years with weak dust transport, e.g., 2005 and 2013. The most obvious discrepancies usually occur in the dust transition period in May-June which in some years appears as a relatively strong secondary peak in the MERRA-2 product. This could be due to difficulties in cloud clearing in the assimilated MODIS product as the ITCZ moves north. To show the overall relationship between MERRA-2 Surface Dust and Cayenne PM_{10}-Dust, in Fig. S7 we show a scatter plot of MERRA-2 Surface Dust and PM_{10}-Dust using data from the entire year and also using only data from the months of the nominal dust season (December through April). The dust season plot shows a strong 1:1 relationship with R^2 = 0.64 with a negligible Y-intercept, 1.1 μg m^{-3}.

To further test the performance of MERRA-2 with African dust transport over the western Atlantic, we made a cursory comparison of Barbados dust measurements over the time period 2002 - 2017 against MERRA-2 monthly means (Fig. 5, bottom). The agreement is excellent, comparable to that obtained with the Cayenne measurements. At Barbados, MERRA-2 accurately captured both the seasonal cycle and mean concentrations over most years but tended to underestimate the peak summer values in some years. Similarly, Buchard et al., (2017) and Randles et al., (2017) found excellent agreement between daily mean MERRA-2 Surface Dust and Barbados measurements over 2010 (see Buchard et al., 2017, Fig. 9 and Randles et al., 2016), Figs. 4.15, 4.16.) The performance that we obtained with MERRA-2 dust is consistent with the results of (Ridley et al., 2016) who, in a comparison with three other frequently-used models, found that MERRA-2 dust AOD better agrees with observations both with regard to seasonality and magnitude.

3.5. Dust deposition to Cayenne

Based on the excellent agreement between PM_{10}-Dust and the MERRA-2 at Cayenne, we estimated dust deposition to a one-degree block centered on Cayenne using the MERRA-2 total (wet-plus-dry) dust deposition product. The average deposition rate over the period 2002 to 2017 is 4.3 g m^{-2} a^{-1}. During the dust season, which is also the rainy season, about 95% of the deposition in the MERRA-2 model is with rain. During summer (e.g., the low-dust season and also the dry season), wet deposition is typically 65 – 75% of total deposition. Based on

©2020 American Geophysical Union. All rights reserved.

MERRA-2, at Cayenne almost a quarter of the annual deposition (23%) occurs in March, the peak dust month, and 89% during the months February through May.

The only directly measured African dust deposition data that is available for comparison in the western Atlantic is that from Prospero et al., (2010) who measured dust deposition at nine sites over the length of Florida for a three-year period in the mid-1990s. They obtained rates in the range of 1.5 to 2.0 g m^{-2} a^{-1}. The lower deposition rates over Florida are consistent with the shorter dust transport season in this region relative to Barbados (Prospero et al., 2010).

Because there are no dust deposition measurements from the Cayenne region that we could use for comparison, we compare the MERRA-2 deposition to Holocene deep-sea sediment dust accumulation rates available in DIRTMAP (Kohfeld & Harrison, 2001). In the central tropical North Atlantic, rates are in the range 1 – 5 g m^{-2} a^{-1}. One core collected on the latitude of Cayenne at about 48°W yields rates in the range of 5 – 10 g m^{-2} a^{-1}. An extensive study of dust input rates to the oceans using the Thorium-232 method (*Thoromap*, Kienast et al., 2016) presents data for the late Holocene (0 – 4ka) in sediments off the NE coast of SA at 45°W, directly east of Cayenne. Of three closely-spaced cores, two yield rates of 2 – 4 g m^{-2} a^{-1} and one of 4 – 8 g m^{-2} a^{-1}. A recent assessment of satellite-based deposition rates to the tropical Atlantic and Caribbean (Yu et al., 2019) yielded rates along the coast of FG in the range of 3.6 – 7.2 g m^{-2} a^{-1}, in good agreement with the MERRA-2 estimates and the sediment deposition rates in the region.

3.6. Dust transport to the Amazon and northern South America

Previous estimates of dust deposition and associated P deposition have been limited to statements of gross deposition rates to the Amazon as a whole. Such estimates are not adequate for assessing the effects of deposition to specific regional ecosystems whose properties will vary greatly across this huge region. Based on the good agreement between MERRA-2 Cayenne dust concentrations and with dust accumulation rates in ocean sediments, we use MERRA-2 to estimate surface dust concentration and dust deposition to SA north of 10°S and east of 75°W). Results are calculated over the period 2002 – 2017 for 5° by 5° blocks arrayed over the region (Fig. 6). This region largely covers the Amazon Basin which, broadly viewed in this context, lies between 5°N and 15°S west of 50°W and extending to the Andes. This area includes the Amazon River which lies mostly between 5°S to 0°N. As we will show, there is little evidence of any substantial dust transport to latitudes below 10°S; indeed, evidence of transport south of 5°S is questionable.

It is clear from Fig. 6 that there is great temporal and spatial variability over the course of the year. To place Fig. 6 into a larger context and to facilitate discussion, we show in Fig. 7 area plots of MERRA-2 seasonal means of surface dust concentration (Fig. 7, top) and dust deposition rates (Fig. 7, bottom) for all of SA. (See also Table 1.)

Focusing first on dust concentrations in Fig. 6, the impact of early-year African dust transport is most evident over the northeast of SA, especially in the Cayenne block which experiences the greatest concentrations of all blocks. The broad peak observed early in the year is clearly associated with the transport to Cayenne as documented in this paper and it is consistent with satellite images of the African dust plume in Spring when the core of the transport plume impacts directly on FG (Chin et al., 2014; Hsu et al., 2012; Yu et al., 2013). This association is also evident in Fig. 7 where MERRA-2 captures the seasonal north-south migration of the African plume over the Atlantic and northern SA.

©2020 American Geophysical Union. All rights reserved.

In contrast, the top tier in Fig. 6 (the 5°N-10°N band) shows a bimodal distribution most clearly seen in the westernmost (75°W-70°W) block. The mid-summer peak is logically associated with the summer transport to the Caribbean, well-documented at Barbados (e.g., Prospero & Lamb, 2003; Prospero & Mayol-Bracero, 2013). The concentrations in the two easterly blocks (which lie mostly over Venezuela) peak at the same time as dust concentrations at Barbados and they are comparable in magnitude as well. This seasonal association can also be seen in Fig. 7 by comparing DJF with JJA. In the top tier in Fig. 6, the early-year peak is clear evidence of the impact of spring dust transport over the northernmost region of SA. The 75°W-70°W block, which lies over northern Colombia and western Venezuela, shows a broad peak in March and April, broadly concurrent with that at Cayenne although only about half as large. The dust season in this region is associated with the calina, a dense haze that has typically been associated with sea salt but which also has been shown to be linked to the presence of mineral dust (Stong, 1961; Zuloaga, 1966). The impact of early-year African dust on air quality is seen in PM_{10} measurements in Colombia (Espinosa et al., 2018; Hernández, 2014). This transport is notable given that the block lies more than 2000 km west of the longitude of Cayenne.

In the 0°N-5°N band (Fig. 6), the seasonal bimodality is still evident but less strong and the March-April peak is more prominent. It is notable that the spring peak stands out even in the most westerly block, over central Colombia east of the Andes (see also Fig. 7, DJF and MAM), which suggests that substantial quantities of African dust survive the transit across the northern reaches of the Amazon Basin or by way of the Caribbean coast. However, dust concentrations are reduced to about a fifth of those at Cayenne. We can assume that much of the dust transiting the Amazon Basin to the west will be removed in orographic precipitation over the Andes as has been observed at a mountain site in Ecuador by Boy & Wilcke, (2008) who specifically attribute the anomalous composition of their precipitation to African dust and suggest that African dust could play an important role in soil chemistry in mountain ecosystems.

In the 5°S-0°N band from 75°W to 45°W (Fig. 6 and Table 1), there is no sign of a summer peak. The early-year peak seen in Cayenne is also evident in the blocks east of 65°W but it is much reduced. The peak is quite prominent in the 50°W to 45°W block because it receives direct transport across the coast. However, in general, the concentrations in the 5°S-0°N band are much reduced compared to those in the 0°N to 5°N band.

The blocks lying in the 10°S-5°S band present a more complex picture. Of these, the blocks east of 50°W show a spring peak that can be reasonably linked to the spring peak seen in Cayenne (see also Fig. 7, DJF and MAM). The blocks west of 55°W are very different. Concentrations are much increased relative to the easterly blocks and there is a very strong bimodal distribution with a prominent peak early in the year and one late in the year. Based on Fig. 7, we might be lead to conclude that this dust is transported from sources in the south of SA. This would be unexpected based on our current knowledge of dust sources in SA. The largest and most active are in Patagonia far to the south, below about 40°S (Crespi-Abril et al., 2018; Gassó et al., 2010; Gassó & Torres, 2019; Prospero et al., 2002). These stand out clearly in Fig. 7 in all seasons. But dust from these sources is generally carried to the east and southeast over the Atlantic (Johnson et al., 2011). Patagonian dust is believed to be an important source of dust transport to the South Atlantic and Antarctic (Li et al., 2010).

In the mid-latitudes (roughly 10°S to 30°S, Fig. 7), a plume-like feature extends north-south that appears largely independent of the sources south of 40°S. In all seasons, but most

©2020 American Geophysical Union. All rights reserved.

distinctly in SON, this plume is seen extending northward from about 30°S mostly between 60°W and 70°W. The centers of activity appear as a series of very small "hot spots" in MERRA-2, most prominently in Fig. 7 in SON. These hot spots have been previously identified in the literature (Bucher & Stein, 2016; Prospero et al., 2002). One of the most notable is Mar Chiquita in Cordoba (62.30°W, 30.40°S), the largest saline lake in SA (Bucher & Stein, 2016). The lake periodically goes through dry cycles at which time it becomes the source of intense dust storms. However, these sources are quite weak compared to dust sources south of 40°S. Nonetheless, a recent study (Della Ceca et al., 2018) shows that mineral dust is a major aerosol component in this region with a maximum in November to February, consistent with the MERRA-2 activity in Fig. 7. Della Ceca *et al.* note that agriculture in this region has increased by 64% since 2000 and is a factor in dust mobilization.

A cursory perusal of Google Earth shows very extensive areas of intense agricultural activity in the region underlying the plume in northern Argentina and extending through Paraguay and into southern Brazil. In contrast, global model studies of anthropogenic dust linked to land use (Chen et al., 2018, 2019; Ginoux et al., 2012) do not show any substantial emissions in the region of the MERRA-2 plume. It is possible that these MERRA-2 sources are an artifact of the response of the source algorithm to the land use classification. Also, MODIS AOD retrievals are less successful over land because of the variable reflectivity of the surface. Consequently, the MERRA-2 assimilation scheme is less effective than over ocean areas.

In order to assess the importance of the agricultural areas cited above as dust sources to the Amazon, we generated a series of HYSPLIT forward trajectories along with frequency analysis for every month of the year. In Fig. S8, we show trajectories for four seasonally representative months (January, April, August, October) calculated for a hypothetical source located at 22°S and 60°W over agricultural lands in Paraguay. In Fig. S9, we do the same for a hypothetical source at 30°S and 61°W, over northern Argentina. It is clear that there can be no substantial dust transport northward from these farming regions to the Amazon region. The trajectories are consistent with our previous understanding that, given the dominant large-scale synoptic picture, transport is predominantly to the south and southeast.

We also note that in the 5°S-10°S band (Fig. 6) in the region of this N-S "surface dust" and "deposition" plumes, the MERRA-2 column dust extinction product (not shown) yields only a weak indication of AOD plumes in MAM and JJA which suggests that the plumes, if any, might be relatively shallow features. It is also possible that the satellite dust retrievals are impacted by BB which is intense and widespread in southern and central Brazil especially during the main burning season, JJA and into SON (Hoelzemann et al., 2009; Martin et al., 2010; Mok et al., 2016; Pereira et al., 2016). Based on satellite aerosol optical depth (Malavelle et al., 2019), the main burning areas in SA are found south of 5°S and west of 53°W. See Fig. S10. In those seasons, MERRA-2 spatial maps of black carbon column extinction show very high values extending from about 5°S into northern Argentina. The model smoke transport path is similar to that of the surface dust plume seen in Fig. 7. MODIS images show dense plumes of smoke being transported to the south in precisely the same region as the MERRA-2 "dust plumes" (Mok et al., 2016). See Fig. S11 for examples. Thus, the anomalous model dust values in JJA and SON may be due, in part, to a smoke-induced bias in MODIS AOD in southern Brazil. However, the origin of the MAM dust peak seen in the blocks west of 55°W in the lowest tier in Fig. 6 remains unexplained since there is no prominent BB early in the year in this region (Malavelle et al., 2019).

©2020 American Geophysical Union. All rights reserved.

There are no other major dust sources in SA that could significantly impact the Amazon. In Fig. 7 (top row) relatively small intense sources are seen in the arid regions that lie along the coasts of Chile and Peru. The transport of these emissions to the east would be blocked by the Andes. An area of intense activity is seen along the north coast of Colombia on the Guajira Peninsula which experiences an arid climate due to its location in the rain shadow of the Sierra Nevada de Santa Marta (altitude 5700 m), the highest mountain range in SA after the Andes. The peninsula is the site of the La Guajira Desert which is most likely the source of the dust seen in MERRA-2. There is substantial dust activity in this desert and this dust is believed to play an important role as a source of nutrients for coastal waters (Andrade & Barton, 2005). However, because of the dominance of the Trade Winds, this desert is unlikely to be a significant source to regions lying to the east.

3.8 Dust deposition to South America

The general trends in transport and deposition seen in Fig. 6 and Fig. 7 suggest that African dust has a modest impact south of the equator wherein lies the heart of the Amazon Basin. The impact of early-year African dust deposition is most evident over northeast SA, most especially in the Cayenne block because of the combined effects of high dust concentrations and the rainy season climate. Moreover, the deposition rates in the 10°S – 5°S band would be further reduced if we exclude the anomalous results obtained for the blocks between 75°W and 50°W.

Table 1 summarizes total dust deposition to each of the five-degree boxes. The deposition rate per unit area (kg ha^{-1}) in each box is presented in Table S1. Total dust deposition to the entire grid extending to 10°S is 10.4 Tg per year. If we exclude the questionable estimates for the 10°S- 5°S band, the total is 8.0 Tg per year. In addition, in Table 1 and Table S1, deposition is separately estimated for the Cayenne winter-spring dust period, nominally December through April, and the Barbados summer dust period, nominally June through September. We do not evaluate seasonal estimates for the band 10°S-5°S because of the questionable results for this latitude band,

North of the equator and west of 60°W, a region the includes the entirety of Venezuela and Colombia and large areas of northern Brazil, the deposition of summer dust is comparable to that of winter-spring dust. East of 60°W to the Atlantic coast, winter-spring dust clearly dominates, especially in the Cayenne block. South of the equator, summer dust is minimally present; winter-spring dust is clearly present and dominant from 65W to the easternmost tip of Brazil.

Viewed broadly, there are large gradients in deposition rates across the domain in Fig. 6 and Fig. 7. The highest rates occur in the northeast coastal region and the northern regions bordering the Caribbean. Deposition to the heart of the Amazon is substantially smaller, presumably because of the removal of dust during transport through the rainy regions of the ITCZ. This contrasts with the suggestion by (Yu et al., 2015b) that deposition should be higher in the central Amazon because of the generally higher rainfall.

Yu et al., estimated deposition to the Amazon Basin using an area somewhat different from ours. Yu's area extends to 12°S whereas we show that there is most likely little transport below about 5°S and that estimates from the region are questionable. In our Table 2, we extract the Yu *et al.*, table (their Table 2) and insert our MERRA-2 estimates along with several other recent estimates. Our result, 8.0 Tg, is the lowest of all the estimates. Note,

©2020 American Geophysical Union. All rights reserved.

however, that the Yu *et al.* estimate, 28 Tg a^{-1}, is associated with a large range, 8 – 48 Tg a^{-1}. Our estimate coincides with the low end of their range.

Our results show strong seasonal changes in deposition. In Table 3 we present our estimates along with those of others including Yu *et al*. (their Table 1). It should be noted that the Yu *et al*. CALIOP estimates are obtained by a distinctly different procedure than the other models. In effect, they estimate the mass input through the north and east sides of their box and subtract the output through the west and south sides of the box. Yu *et al.* find no significant deposition in JJA and SON using CALIOP although using MODIS they find a substantial deposition in these seasons. All the other studies shown in Table 3 found substantial deposition in JJA and SON.

Gläser et al. (2015b) estimated dust transport and deposition to SA using the fifth generation European Centre for Medium Range Weather Forecast-Hamburg model (ECHAM5)/Modular Earth Submodel System (MESSy) Atmospheric Chemistry model. They obtained estimates of deposition by combining correlation analyses of Eulerian dust fluxes and Lagrangian trajectory calculations. These yielded two values 34.3 Tg a^{-1} and 11.4 Tg a^{-1} (Table 2). (The rates per unit area in Table 2 are calculated based on our estimate of the area depicted in their Fig. 1a.) The Eularian rates in Glaser are substantially higher than ours while the Lagrangian rate is quite similar. Glaser *et al.* also estimated dust deposition in each of the four seasons (Table 3). They too found a high deposition rate in JJA, comparable to that in MAM., and also a substantial deposition rate in SON.

Herbert et al. (2018) used the Global Model of Aerosol Processes (GLOMAP) coupled with the chemical transport model TOMCAT to simulate the emission, transport, and deposition of dust-borne phosphorus to the surface. They obtained a dust deposition rate of 32.3 Tg dust per year deposited to SA. This includes the significant deposition in Argentina which clearly is due to dust from local sources. Assuming that dust is deposited to approximately the same areas as in Yu *et al.*, the deposition rate of dust would be 34 kg ha^{-1} a^{-1}. On the basis of Fig. 2 in Herbert et al., we can roughly estimate deposition to the amazon basin using the rate range indicated on the color scale, 1 – 5 g dust m^{-2} a^{-1}. This yields a total deposition rate range of 4.2 to 21 Tg dust per year and a P deposition rate of 10 to 50 gP m^{-2} a^{-1}. A comparison of these estimated rates with those in Table 3 shows that they fall into the general range of model results and that they are higher than that obtained by us with MERRA-2 although the low end of the range is only slightly higher than our estimated rate, 9 gP m^{-2} a^{-1}.

Our seasonal deposition trend is similar to that found by Ridley et al. (2016) who used the GEOS-Chem model, the same transport model as that used in MERRA-2. They also find a substantial summer transport. However, our estimates are lower than theirs, overall 60% of their seasonal values except for SON. The difference in our rates is most likely because the transport model in MERRA-2 is adjusted by assimilating MODIS AOD measurements which should improve the performance of the model.

4. DISCUSSION

4.1 Dust transport and temporal-spatial variability

MERRA-2 shows considerable temporal and spatial variability in both the concentration and deposition of dust across SA. The impact of African spring dust transport is greatest to the northern and northeast regions of SA while comparatively little penetrates deeply into the Amazon Basin south of the equator. Gläser et al. (2015a) in their trajectory-based study show the same general pattern of deposition with very little deposited to the Amazon Basin.

©2020 American Geophysical Union. All rights reserved.

We can get a better sense of the factors controlling transport to the southwest in the Basin by comparing our Cayenne measurements with those made at the Amazon Tall Tower Observatory (ATTO: 2.14°S, 59.00°W; 130 m. a.s.l). ATTO, operated under a German and Brazilian partnership Andreae et al. (2015), is located in a pristine rain forest in the central Amazon, about 150 km northeast of Manaus, Brazil, and 1000 km southwest (at 225 degrees) of Cayenne (Andreae et al., 2015; Pöhlker et al., 2016, 2018, 2019). See Fig. 1. Early in the year, HYSPLIT forward trajectories from Cayenne consistently fall into a tight pattern to the SW (see Fig. S12) that would carry air parcels directly to the ATTO region and into the heart of the Amazon Basin.

Moran-Zuloaga et al. (2018) present results of un-speciated coarse mode (1-10 μm diameter) aerosol over the period 2014 to 2016 (see their Fig. 2). Comparing our Fig. 2 with their Fig. 2, one sees a correspondence in the timing of some PM_{10} peaks at Cayenne with coarse mode aerosol at ATTO which suggests that coarse mode aerosol at ATTO is driven by African dust advected through the Cayenne region. However, the peak amplitudes at ATTO are often greatly reduced and the timing is often shifted to a couple of days later as might be expected because of the travel time between sites. A similar relationship can be seen between the ATTO measurements in 2015 and 2016 (Rizzolo et al., 2017) and the times series of PM_{10} shown in our Fig. S4. In many cases, there are no corresponding peaks to be seen in the ATTO record, in many cases, most likely due to removal by rain. These omissions are more common late in spring, a time when the forward trajectories from Cayenne take on a more westerly component (see Fig. S12). Many aspects of the relationship between aerosol properties at ATTO and the large-scale meteorology are addressed in considerable detail in Moran-Zuloaga et al. (2018) and Pöhlker *et al.*, (2016, 2018, 2019).

Unfortunately, other than sporadic measurements, there are very few dust-specific time-series elsewhere in the Amazon Basin that could serve to test the MERRA-2 results. The most extensive data are presented in (Mahowald et al., 2005a, 2008) who summarize multi-month data from four sites: Balbina, 2°S, 60°W; Santarem, 2°S, 5°W; Alta Floresta, 10°S, 57°W; Rondonia; 11°S, 62°W. The data from Mahowald *et al.* (2005) are in agreement with the general picture presented in our MERRA-2 results, but our measured concentrations are substantially lower. This difference may be due in part to considerable year-to-year variability in the MERRA-2 derived concentrations for these sites, a reflection of the strong control that the ITCZ has over transport to the lower latitudes in the Amazon region. Also, the MERRA-2 results were run for the period 2002 to 2017 whereas the Mahowald data were obtained in years prior to 2002 as part of the Large Scale Biosphere-Atmosphere Experiment in Amazonia (LBA, Artaxo et al., 2002).

Although our major interest lies with the winter-spring transport to Cayenne, there is also a minor advection of dust in summer and fall as previously noted (Figs. 2, 4, S4). The low-dust season is associated with seasonal movement of the ITCZ which results in a change in Cayenne back trajectories and a shift to paths over the central South Atlantic (Fig. S3). It is therefore assumed that the dust and other non-marine aerosols during this period originate from southern Africa as discussed in Barkley et al. (2019). Beginning in May and continuing through the year, BB is intense between the latitudes of 10S to 20 S. There are also active dust sources south of 20S in Namibia, Botswana and South Africa (Prospero et al., 2002). Although these sources are small compared to North Africa, they are nonetheless significant in that they are the only sources that impact the mid-latitude South Atlantic. The impact of these sources can be seen in the MERRA-2 surface dust distribution plots (Fig. 7, top), which

©2020 American Geophysical Union. All rights reserved.

show dust carried to eastern Brazil and the NE coast of SA, most notably in SON, albeit at very low concentrations.

4.2 Phosphorus deposition with dust

We estimate dust P (Dust-P) deposition to the Amazon basin by multiplying the dust deposition by the P concentration in dust. The average P concentration in upper-continental crust is 660 ppm (Rudnick & Gao, 2003). Various values have been reported for P in mineral particles: African Sahel soils, a suspected source for Cayenne dust, 780 ppm (Bristow et al., 2010), African dust collected at Miami and Barbados, 880 ppm (Zamora et al., 2013), aerosols collected at Cayenne, 1080 ppm (Barkley et al., 2019). The elevated P concentrations shown in Barkley *et al.* are likely due to co-transported African BB aerosol. Using MERRA-2, we calculated the total annual dust deposition to the area delineated in Fig. 1. (Note that our area is configured somewhat differently from that in Yu et al. which is also marginally larger, about 10%). Using a value of 780 ppm P in dust, the same as in Yu *et al.*, we obtain a total P deposition of 0.0056 Tg P a^{-1} for an average rate of 7.4 g P ha^{-1} a^{-1}, much lower than all the other estimates shown in Table 2. If we use the P concentration from Barkley *et al.*, 1080 ppm, the average rate would be 10.2 g P ha^{-1} a^{-1}.

From Table 1, we can estimate P deposition to each of the five-degree boxes by assuming, for convenience, a P concentration in dust of 1000 ppm. The deposition of Dust-P to each box is summarized in Table S2. The highest deposition rate is in the 5° box that includes Cayenne, 43 g P ha^{-1} a^{-1}. Excluding all blocks below 5°S, which do not appear to be substantially impacted by African sources and where MERRA-2 results are questionable, the lowest deposition rate in the extreme western block in the 5°S - 0°N band, 10 g P ha^{-1} a^{-1}, is a factor of four lower than the Cayenne block. Nonetheless, despite the differences in dust sources and the seasonality, the deposition rates across the northern Amazon tend to fall into a relatively narrow range in part because of the impact of transport by two routes, predominantly from the east in winter-spring and from the north in summer.

There are few measurements of atmospheric deposition in SA. In a recent review of global precipitation chemistry (Vet et al., 2014), no sites in SA followed protocols that qualified for inclusion. A compilation (Tipping et al., 2014) shows data only for 15 sites in Central and South America but only six measure total P.

Moreover, the P source assessment is difficult because of widespread BB, especially in the Amazon Basin. Smoke contains substantial concentrations of P (Anderson et al., 2010; Ito et al., 2019; Mahowald *et al.*, 2008, 2017; Myriokefalitakis *et al.*, 2016; Wang *et al.*, 2014). Thus, measurements of deposited P can be dominated by locally-derived smoke-P that will mask any imported P especially in the central and southern regions of the basin where burning is most intense. Three sites in Brazil yield rates ranging from 180 to 370 g P ha^{-1} a^{-1}. A site in Costa Rica yielded a similar value but two in Venezuela yielded much higher values, 1100g and 1680 g P ha^{-1} a^{-1}. These clearly reflect the effects of local BB sources.

Das et al. (2013) measured P deposition in rainfall at a site on the Yucatan Peninsula which should be heavily impacted by African dust in the summer months at rates comparable to those in the states in SA bordering the Caribbean (see Fig. 6). They assessed the contribution of long-distance dust transport to the P inputs using MODIS and the MATCH model and estimated the dust contributed 46 g P ha^{-1} a^{-1}, a value about twice that listed in Table 1 for the 5-degree boxes bordering the Caribbean.

©2020 American Geophysical Union. All rights reserved.

4.3 Phosphorous and African biomass-burning smoke

Recently, Barkley *et al.*, based on their measurements of dust and P in aerosols at Cayenne, suggested that the transport of BB-P from African could provide significant quantities of P to SA. As noted above, the filters collected at Cayenne always show signs of gray-black aerosol (see Barkley *et al.*, Fig. S5, S8). The MERRA-2 black carbon model product (Fig. S13) centered on Cayenne yields a bimodal annual cycle with a maximum in September, around the time of the broad peak in PM_{10} seen in Fig. 4 (days 260 – 280, September-October). The gray color on filters is most intense in summer, when dust concentrations are at their lowest, and serves as evidence of the dominant presence of BB products in the Trade Winds. Over Cayenne in summer, CALIOP frequently shows aerosol plumes wherein the aerosol characterization algorithm identifies smoke as a major component (Barkley *et al.*, 2019). A similar seasonal impact of BB from sources in southern Africa are also noted at ATTO (Saturno et al., 2018). More recently, de Oliveira et al. (2019) reported on a 12-year analysis (2005 to 2016) of atmospheric aerosol optical properties over easternmost Brazil (i.e., in the easternmost block in the bottom tier of Fig. 6) and showed the strong and persistent impact of BB transported from southern Africa. They obtain an AOD peak in September-October that coincides with the PM_{10} peak seen in Fig. 4. Barkley *et al.* conclude that BB smoke from southern Africa is a significant source of total P, comparable to the dust source and that it is the dominant source of imported soluble P supplied to the Amazon.

4.4 Cayenne dust and African climate

The 50-year record of African dust transport to Barbados shows great changes with time that can be linked to climate variability in Africa, most visibly to droughts in the early 1970s and again in the 1980s (Propero and Nees, 1977, Prospero & Lamb, 2003). Over much of the record, annual dust transport to the Caribbean appeared to be inversely linked to prior-year rainfall in the Sahel. Sahel rainfall can serve as a proxy for larger-scale meteorological and climatological conditions over West Africa (Cuevas et al., 2017; Evan et al., 2016; Nicholson, 2015; Sheen et al., 2017). The negative relationship is consistent with the expectation that rains would tend to stabilize soils and encourage plant growth which, in turn, would further protect against deflation. More recently other factors have been suggested, most notably changes in wind speeds in the source areas (Ridley *et al.*, 2014). Recently, Yu *et al.* used CALIOP to examine the relationship between dust transport and deposition to the Amazon in terms of Sahel rainfall. Over the period 2007 to 2013, they found a strong negative correlation between prior-year rainfall and dust mass flux and deposition, a result similar to what was found at Barbados (Prospero and Lamb, 2003).

Here we examine the relationship between Cayenne seasonal PM_{10}-Dust concentrations and the Sahel precipitation index (SPI), the same used by Prospero and Lamb and by Yu *et al.* (SPI, http://www.jisao.washington.edu/data_sets/sahel/; doi:10.6069/H5MW2F2Q). We separately examined the two dust seasons, DJF and MAM. In each season, we plotted two cases: dust concentrations against prior-year SPI and against current year SPI. The season DJF yielded no significant correlations: $R^2 = 0.063$ against current year SPI and $R^2 = 0.002$ against prior-year SPI. In contrast, MAM yields a modest negative correlation ($R^2 = 0.16$) against previous year SPI (Fig. 8b). This is consistent with the results obtained at Barbados (Prospero and Lamb, 2003) and by Yu *et al.* for the Amazon. In contrast, the MAM period yields a modest positive correlation ($R^2 = 0.24$) with current-year SPI (Fig. 8a). This is surprising because the rainy season in the Sahel is linked to the West African monsoon which occurs later in the year, after the spring dust season.

©2020 American Geophysical Union. All rights reserved.

We further examined the relationship to SPI by comparing the MERRA-2 surface dust concentrations (MERRA-2 DUSMASS) obtained in a 2-by-2 degree block centered on Cayenne. We found the same, but stronger, negative relationship between MAM model dust and prior-year SPI ($R^2 = 0.405$) but none against current-year ($R^2 = 0.006$). The disparity between the model result and the Cayenne measurements might be linked to the way in which we subtract a fixed "background" PM_{10} value from total PM_{10} to estimate PM_{10}-Dust. The background aerosol at Cayenne is dominated by sea salt; inter-annual changes in sea-salt concentrations could introduce considerable variability.

To place the Cayenne MERRA-2 results in a larger context, we created scatter plots similar to Fig. 8 using an array of 5-by-5 degree blocks centered on the Cayenne block (Fig. S14). In each case, in MAM there was a clear inverse relationship between MERRA-surface dust and previous-year SPI. The relationship was strongest for the more northerly and easterly blocks. It was weakest for the ATTO block. In the same way, we also examined scatter plots against current year SPI (not shown) and found no persuasive relationship.

Although not shown here, we also examined the relationship between MERRA-2 total dust deposition (DUDPWTSUM) and SPI. Here, too, we found a strong negative correlation (R^2= 0.323) similar to that obtained for dust concentration. We also looked at MERRA-2 total column dust (DUCMASS) and SPI and obtained the same result as with MERRA-2 surface dust and we obtained essentially identical R^2 values. This implies that the surface dust concentration is closely linked to column dust loads.

Broadly speaking, we find a similar inverse relationship between dust transport and SPI as that found by Yu et al. However, our results are not directly comparable. First of all, Yu et al. measured the difference between the boundary fluxes into, and out of, the entire region. This yields the gross Basin deposition. Also, our time span is twice as long. Nonetheless, both studies suggest a strong link to Sahel precipitation. Our work shows a particularly strong relationship between MAM dust transport and SPI but nothing between DJF dust and SPI as implied by Yu et al. Also, we find a looser relationship than did Yu et al., as suggested by the R^2 values of our respective regressions. Moreover, we find that the relationship is strongly evident only in the northeastern regions of our study area. In contrast, the result in Yu *et al.* implies that the effect impacts a large area of the Amazon Basin.

4.5 Linking specific African dust sources to impacts in South America

There have been many efforts to identify the most intensely active dust source regions in North Africa (e.g., Evan et al., 2015; Formenti et al., 2011; Schepanski et al., 2017). The Bodele Depression in northern Chad has often been identified as one of the most intense and persistently active sources on Earth (Warren et al., 2007). It has been specifically cited as a major source of dust transported to South America (Ben-Ami et al., 2010; Koren et al., 2006) and it is suggested to be the most important source of Dust-P transported to the Amazon (Bristow *et al.*, 2010). The back trajectory frequency plots for March at 2000 m and 3000 m altitude (Fig. S3) are, in part, consistent with transport form the Bodele but also from a wider region in West Africa including the Sahel and the southern Sahara. Indeed, the importance of the Bodele is yet to be established in a quantitative way. A number of studies of the elemental and isotopic composition of summer-season dust transported to the Caribbean (Bozlaker et al., 2017; Kumar et al., 2018; Pourmand et al., 2014; Zhao et al., 2018) have shown that dust isotopic signatures exclude the Bodele as a source. Gläser et al., (2015b), in their trajectory study, could find no strong evidence that the Bodele was a significant source. They attribute the absence of an impact from the Bodele to the fact that trajectories from the Bodele tend to

©2020 American Geophysical Union. All rights reserved.

enter the ITCZ over the mid-Atlantic where rain will remove dust. This is consistent with the observation of high concentrations of freshwater diatoms in mid-Atlantic sediments in this region (Romero et al., 1999).

Glaser *et al.* conclude that the sources with the greatest impact on SA were those located in Mali, Mauritania, and Algeria, especially those in the region stretching from Central Algeria at 5°E, 30°N to the eastern part of Mauritania at 10°W, 20°N. They also find that most dust reaching the Caribbean in summer is emitted from this same general region. These same regions were identified as the sources of summer dust collect at Barbados based on the elemental and isotopic composition of the dust compared to those of hypothesized source regions in North Africa (Bozlaker *et al.*, 2017). However, it should be noted that these works primarily focus on summer dust; there are few isotopic studies of winter-spring dust transport when transport from the Bodele would be most favored.

4.6 African dust and air quality in South America

Although our research is motivated by our interest in the impact of dust on the Amazon, it is relevant to other issues including air quality and human health. There is considerable evidence that mineral dust can have a negative impact on human health (e.g., Querol et al., 2019; Zhang et al., 2016). The MERRA-2 model suggests that sporadically high values of dust could lead to health impacts as previously noted (Prospero *et al.*, 2014). Aside from dust events, the air quality in Cayenne is generally very good because of strong ocean winds and low emissions from local sources. In contrast, the urban complexes in the northern states of SA will likely have substantial sources of local and regional emissions which, when coupled with dust incursions, could lead to frequent exceedances of the WHO PM_{10} 24-hour guideline, 50 µg m^{-3}. Moreover, many regions in northern SA (e.g., Colombia, Venezuela, Guyana, Surinam) will be doubly impacted by African dust: by the winter-spring dust that affects Cayenne and also by the summer dust that impacts Barbados. As we have shown, air quality measurements of PM_{10} can be used to quantify dust impacts and, thus, to improve forecast tools. These could then be used to issue air quality alerts in anticipation of major dust incursions.

5 Conclusions

Our measurements of mineral dust and PM_{10} in Cayenne show that large quantities of African dust are routinely transported to SA in boreal winter and spring. MERRA-2 model deposition estimates are considerably lower than those obtained in previous studies that had been based on various satellite products and atmospheric transport models. Our results raise questions about the magnitude and importance of African dust as a source of nutrients, especially phosphorus. Moreover, it has been suggested that the transport of dust-P to South America would serve to replenish P and other nutrients that are lost through the transport of biomass burning smoke out of the major burning regions. Here we show that very little African dust reaches the major fire areas which are mainly located in southwestern Brazil.

However, we caution that our estimates are based on the results of a model, MERRA-2 which we show to be well-validated by long-term measurements at Cayenne and Barbados. All other models yield substantially greater transport. The large range of model estimates in Table 3 suggests that there are large uncertainties in estimating transport and, consequently, deposition. Because of the absence of dust deposition measurements in SA, we cannot test the deposition component of MERRA-2. A more solid assessment can only be achieved by initiating a greater range of aerosol and precipitation measurements made in a wide range of

©2020 American Geophysical Union. All rights reserved.

environments. This will require studies in more regions in SA and carried out over multi-year time periods. There is a growing recognition of this need. Organizing efforts are underway to develop a more cohesive and sustained community of atmospheric scientists in the Latin America–Caribbean region to address the pressing issues of air quality and climate change (Andrade-Flores et al., 2016).

While the focus of this paper has been on dust, recent work suggests that the transport of BB products from southern Africa could serve as a significant source of P to soils in SA. Because this transport takes place during the SA dry season, BB is more likely to penetrate deep into the Amazon rather than dust which is transported mainly in the wet season. In contrast to the P in dust, the P in BB products is highly soluble and, once deposited, would be immediately available for uptake in biomass (Barkley *et al.*, 2019). Therefore, it is important to also monitor the BB products transported from Africa. To this end, it will be necessary to make such measurements at coastal locations where samples will not be compromised by smoke from BB sources in SA.

Cayenne is the ideal location for the study of winter-spring transport to SA. In effect, it is the gateway for African aerosol transport to equatorial SA and to the heart of the Amazon Basin. During the dust season, the ATTO facility near Manaus is often located directly in the trajectory plume from Cayenne and about 1000 km downwind (Pohlker et al., 2019). The pairing of measurements at Cayenne with those made at ATTO would be ideal for quantifying this transport and for characterizing the atmospheric processing of dust and BB aerosol in transit.

To better monitor transport from Africa during summer, a study site along the coast of Brazil between 5°S – 10°S would be ideal (Moran-Zuloaga et al., 2018; de Oliveira *et al.*, 2019; Pohlker et al., 2019). Finally, measurements made along the coast of Argentina between about 40°S - 45°S would provide valuable information on the export of mineral dust and BB aerosol from southern SA to the South Atlantic. These data would be important for quantifying the transport of P and Fe to the Southern Ocean, information vitally needed to assess the impact of SA sources on the primary productivity of this data-poor ocean region (Myriokefalitakis et al., 2016).

Our study shows that African dust transport to northeastern SA is linked to climate in North Africa, specifically to precipitation in the Sahel. Consequently, climate change could affect the location and intensity of dust emissions in Africa and the subsequent long-range transport to SA (e.g., Albani et al., 2019; Evan *et al.*, 2016). Therefore, there is an urgent need to implement decade-long studies in SA to monitor changes over time. However, as pointed out by Andrade *et al.*, the major impediment is a lack of resources. Although there are many scientists in the region who have received advanced training, many in developed countries, they cannot find adequate research positions or obtain funding in their home countries.

Acknowledgments
We thank ATMO Guyane (https:// www.atmo-guyane.org/) for collecting filter samples and maintaining the field site in Cayenne, French Guiana. C.J.G. acknowledges funding provided by the Provost Award from the University of Miami. A.E.B. and C.J.G. acknowledge funding from the University of Miami Advanced Study of the Americas (UMIA). The authors acknowledge the National Oceanic and Atmospheric Administration (NOAA) Air Resources Laboratory (ARL) for the provision of the HYSPLIT transport and dispersion model and READY website (http://www.ready.noaa.gov). We thank the National Aeronautics and Space

©2020 American Geophysical Union. All rights reserved.

Administration (NASA) for making the CALIOP and MERRA-2 data available to the scientific community. We thank the University of Washington Joint Institute for the Study of the Atmosphere and Ocean (JISAO) for the use of Sahel precipitation data. The authors state that they have no conflicts of interest. Cayenne aerosol filter data for the year 2014 is available at the University of Miami Data Repository under https://doi.org/..... and the Barbados data at https://.... Cayenne PM_{10} data can be downloaded at the ATMO data repository web site: https://data-atmo-guyane.opendata.arcgis.com/

REFERENCES

Adams, A. M., Prospero, J. M., & Zhang, C. (2012). CALIPSO-derived three-dimensional structure of aerosol over the Atlantic Basin and adjacent continents. *Journal of Climate, 25*(19), 6862-6879.

Albani, S., & Mahowald, N. M. (2019). Paleodust Insights into Dust Impacts on Climate. *Journal of Climate, 32*(22), 7897-7913.

Anderson, L. D., Faul, K. L., & Paytan, A. (2010). Phosphorus associations in aerosols: What can they tell us about P bioavailability? *Marine Chemistry, 120*(1), 44-56. doi:https://doi.org/10.1016/j.marchem.2009.04.008

Andrade-Flores, M., Rojas, N., Melamed, M. L., Mayol-Bracero, O. L., et al., (2016). Fostering a Collaborative Atmospheric Chemistry Research Community in the Latin America and Caribbean Region. *Bulletin of the American Meteorological Society, 97*(10), 1929-1939. doi:10.1175/bams-d-14-00267.1

Andrade, C. A., & Barton, E. D. J. C. S. R. (2005). The Guajira upwelling system. *25*(9), 1003-1022.

Andreae, M. O., Acevedo, O. C., Araùjo, A., Artaxo, P., Barbosa, C. G. G., Barbosa, H. M. J., *et al.,* (2015). The Amazon Tall Tower Observatory (ATTO): Overview of pilot measurements on ecosystem ecology, meteorology, trace gases, and aerosols. *Atmospheric Chemistry and Physics, 15*(18), 10723-10776. doi:10.5194/acp-15-10723-2015

Ansmann, A., Baars, H., Tesche, M., Müller, D., Althausen, D., Engelmann, R., et al. (2009). Dust and smoke transport from Africa to South America: Lidar profiling over Cape Verde and the Amazon rainforest. *Geophysical Research Letters, 36*(11). doi:10.1029/2009GL037923

Arimoto, R., Duce, R., Ray, B., Ellis Jr, W., Cullen, J., & Merrill, J. (1995). Trace elements in the atmosphere over the North Atlantic. *Journal of Geophysical Research: Atmospheres, 100*(D1), 1199-1213.

Artaxo, P., Martins, J. V., Yamasoe, M. A., Procópio, A. S., Pauliquevis, T. M., Andreae, M. O., . . . Leal, A. M. C. (2002). Physical and chemical properties of aerosols in the wet and dry seasons in Rondônia, Amazonia. *Journal of Geophysical Research: Atmospheres, 107*(D20), LBA 49-41-LBA 49-14. doi:doi:10.1029/2001JD000666

Artaxo, P., Rizzo, L. V., Brito, J. F., Barbosa, H. M. J., Arana, A., Sena, E. T., . . . Andreae, M. O. (2013). Atmospheric aerosols in Amazonia and land use change: from natural biogenic to biomass burning conditions. *Faraday Discussions, 165*(0), 203-235. doi:10.1039/C3FD00052D

Baars, H., Ansmann, A., Althausen, D., Engelmann, R., Artaxo, P., Pauliquevis, T., & Souza, R. (2011). Further evidence for significant smoke transport from Africa to Amazonia. *Geophys. Res. Lett., 38*(20), L20802. doi:10.1029/2011gl049200

Barkley, A. E., Prospero, J. M., Mahowald, N., Hamilton, D. S., Popendorf, K. J., Oehlert, A. M., . . . Gaston, C. J. (2019). African biomass burning is a substantial source of phosphorus deposition to the Amazon, Tropical Atlantic Ocean, and Southern Ocean. *Proceedings of the National Academy of Sciences, 116*(33), 16216-16221. doi:10.1073/pnas.1906091116

Ben-Ami, Y., Koren, I., & Altaratz, O. (2009). Patterns of North African dust transport over the Atlantic: winter vs. summer, based on CALIPSO first year data. *Atmospheric Chemistry and Physics, 9*(20), 7867-7875.

Ben-Ami, Y., Koren, I., Rudich, Y., Artaxo, P., Martin, S. T., & Andreae, M. O. (2010). Transport of North African dust from the Bodélé depression to the Amazon Basin: A case study. *Atmospheric Chemistry and Physics, 10*(16), 7533-7544. doi:10.5194/acp-10-7533-2010

Bovolo, C. I., Pereira, R., Parkin, G., Kilsby, C., & Wagner, T. (2012). Fine-scale regional climate patterns in the Guianas, tropical South America, based on observations and reanalysis data. *International Journal of Climatology, 32*(11), 1665-1689. doi:10.1002/joc.2387

Boy, J., & Wilcke, W. (2008). Tropical Andean forest derives calcium and magnesium from Saharan dust. *Global Biogeochemical Cycles, 22*(1). doi:doi:10.1029/2007GB002960

Bozlaker, A., Prospero, J. M., Price, J., & Chellam, S. (2017). Linking Barbados Mineral Dust Aerosols to North African Sources Using Elemental Composition and Radiogenic Sr, Nd, and Pb Isotope Signatures. *Journal of Geophysical Research: Atmospheres*, n/a-n/a. doi:10.1002/2017JD027505

©2020 American Geophysical Union. All rights reserved.

Bozlaker, A., Prospero, J. M., Price, J., & Chellam, S. (2019). Identifying and Quantifying the Impacts of Advected North African Dust on the Concentration and Composition of Airborne Fine Particulate Matter in Houston and Galveston, Texas. *Journal of Geophysical Research: Atmospheres, n/a*(n/a). doi:10.1029/2019jd030792

Brienen, R. J. W., Phillips, O. L., Feldpausch, T. R., Gloor, E., Baker, T. R., Lloyd, J., . . . Zagt, R. J. (2015). Long-term decline of the Amazon carbon sink. *Nature, 519*, 344. doi:10.1038/nature14283 https://www.nature.com/articles/nature14283#supplementary-information

Bristow, C. S., Hudson-Edwards, K. A., & Chappell, A. (2010). Fertilizing the Amazon and equatorial Atlantic with West African dust. *Geophysical Research Letters, 37*(14). doi:10.1029/2010GL043486

Buchard, V., Randles, C. A., Silva, A. M. d., Darmenov, A., Colarco, P. R., Govindaraju, R., . . . Yu, H. (2017). The MERRA-2 Aerosol Reanalysis, 1980 Onward. Part II: Evaluation and Case Studies. *Journal of Climate, 30*(17), 6851-6872. doi:10.1175/jcli-d-16-0613.1

Bucher, E. H., & Stein, A. F. (2016). Large Salt Dust Storms Follow a 30-Year Rainfall Cycle in the Mar Chiquita Lake (Córdoba, Argentina). *PLOS ONE, 11*(6), e0156672. doi:10.1371/journal.pone.0156672

Carlson, T. N. (2016). The Saharan Elevated Mixed Layer and its Aerosol Optical Depth. *The Open Atmospheric Science Journal, 10*(1).

Carlson, T. N., & Prospero, J. M. (1972). The Large-Scale Movement of Saharan Air Outbreaks over the Northern Equatorial Atlantic. *Journal of Applied Meteorology, 11*(2), 283-297.

Chen, S., Jiang, N., Huang, J., Xu, X., Zhang, H., Zang, Z., . . . Feng, T. (2018). Quantifying contributions of natural and anthropogenic dust emission from different climatic regions. *Atmospheric Environment, 191*, 94-104. doi:https://doi.org/10.1016/j.atmosenv.2018.07.043

Chen, S., Jiang, N., Huang, J., Zang, Z., Guan, X., Ma, X., . . . Zhang, Y. (2019). Estimations of indirect and direct anthropogenic dust emission at the global scale. *Atmospheric Environment, 200*, 50-60. doi:https://doi.org/10.1016/j.atmosenv.2018.11.063

Chin, M., Diehl, T., Tan, Q., Prospero, J., Kahn, R., Remer, L., . . . Geogdzhayev, I. (2014). Multi-decadal aerosol variations from 1980 to 2009: a perspective from observations and a global model.

Chin, M., Diehl, T., Tan, Q., Prospero, J. M., Kahn, R. A., Remer, L. A., . . . Zhao, X. P. (2014). Multi-decadal aerosol variations from 1980 to 2009: a perspective from observations and a global model. *Atmos. Chem. Phys., 14*(7), 3657-3690. doi:10.5194/acp-14-3657-2014

Chin, M., Ginoux, P., Kinne, S., Torres, O., Holben, B. N., Duncan, B. N., . . . Nakajima, T. (2002). Tropospheric aerosol optical thickness from the GOCART model and comparisons with satellite and Sun photometer measurements. *Journal of the atmospheric sciences, 59*(3), 461-483.

Colarco, P., da Silva, A., Chin, M., & Diehl, T. (2010). Online simulations of global aerosol distributions in the NASA GEOS-4 model and comparisons to satellite and ground-based aerosol optical depth. *Journal of Geophysical Research: Atmospheres, 115*(D14).

Crespi-Abril, A. C., Soria, G., De Cian, A., & López-Moreno, C. (2018). Roaring forties: An analysis of a decadal series of data of dust in Northern Patagonia. *Atmospheric Environment, 177*, 111-119. doi:https://doi.org/10.1016/j.atmosenv.2017.11.019

Cuevas, E., Gómez-Peláez, A. J., Rodríguez, S., Terradellas, E., Basart, S., García, R. D., . . . Alonso-Pérez, S. (2017). The pulsating nature of large-scale Saharan dust transport as a result of interplays between mid-latitude Rossby waves and the North African Dipole Intensity. *Atmospheric Environment, 167*, 586-602. doi:https://doi.org/10.1016/j.atmosenv.2017.08.059

Das, R., Evan, A., & Lawrence, D. (2013). Contributions of long-distance dust transport to atmospheric P inputs in the Yucatan Peninsula. *Global Biogeochemical Cycles, 27*(1), 167-175. doi:10.1029/2012GB004420

Das, R., Lawrence, D., D'Odorico, P., & DeLonge, M. (2011). Impact of land use change on atmospheric P inputs in a tropical dry forest. *Journal of Geophysical Research: Biogeosciences, 116*(G1). doi:10.1029/2010jg001403

de Oliveira, A. M., Souza, C. T., de Oliveira, N. P. M., Melo, A. K. S., Lopes, F. J. S., Landulfo, E., . . . Hoelzemann, J. J. (2019). Analysis of atmospheric aerosol optical properties in the Northeast Brazilian atmosphere with remote sensing data from MODIS and CALIOP/CALIPSO satellites, AERONET photometers and a ground-based lidar. *Atmosphere, 10*(10). doi:10.3390/atmos10100594

Delany, A. C., Claire Delany, A., Parkin, D. W., Griffin, J. J., Goldberg, E. D., & Reimann, B. E. F. (1967). Airborne dust collected at Barbados. *Geochimica et Cosmochimica Acta, 31*(5), 885-909. doi:10.1016/s0016-7037(67)80037-1

Della Ceca, L. S., García Ferreyra, M. F., Lyapustin, A., Chudnovsky, A., Otero, L., Carreras, H., & Barnaba, F. (2018). Satellite-based view of the aerosol spatial and temporal variability in the Córdoba region (Argentina) using over ten years of high-resolution data. *ISPRS Journal of Photogrammetry and Remote Sensing, 145*, 250-267. doi:https://doi.org/10.1016/j.isprsjprs.2018.08.016

Espinosa, J. F. M., Herrera, L. C. P., & Cerón, L. C. B. (2018). Estudio de una intrusión de polvo sahariano en la atmósfera de Colombia. *Revista Ingenierías Universidad de Medellín, 17*(32).

©2020 American Geophysical Union. All rights reserved.

Evan, A. T., Fiedler, S., Zhao, C., Menut, L., Schepanski, K., Flamant, C., & Doherty, O. (2015). Derivation of an observation-based map of North African dust emission. *Aeolian Research, 16*, 153-162. doi:10.1016/j.aeolia.2015.01.001

Evan, A. T., Flamant, C., Gaetani, M., & Guichard, F. (2016). The past, present and future of African dust. *Nature, 531*, 493. doi:10.1038/nature17149

Formenti, P., Andreae, M. O., Lange, L., Roberts, G., Cafmeyer, J., Rajta, I., . . . Lelieveld, J. (2001). Saharan dust in Brazil and Suriname during the Large-Scale Biosphere-Atmosphere Experiment in Amazonia (LBA) - Cooperative LBA Regional Experiment (CLAIRE) in March 1998. *Journal of Geophysical Research Atmospheres, 106*(D14), 14919-14934. doi:10.1029/2000JD900827

Formenti, P., Schütz, L., Balkanski, Y., Desboeufs, K., Ebert, M., Kandler, K., . . . Zhang, D. (2011). Recent progress in understanding physical and chemical properties of African and Asian mineral dust. *Atmos. Chem. Phys., 11*(16), 8231-8256. doi:10.5194/acp-11-8231-2011

Gassó, S., Stein, A., Marino, F., Castellano, E., Udisti, R., & Ceratto, J. (2010). A combined observational and modeling approach to study modern dust transport from the Patagonia desert to East Antarctica. *Atmos. Chem. Phys., 10*(17), 8287-8303. doi:10.5194/acp-10-8287-2010

Gassó, S., & Torres, O. (2019). Temporal Characterization of Dust Activity in the Central Patagonia Desert (years 1964-2017). *Journal of Geophysical Research: Atmospheres, 0*(ja). doi:10.1029/2018jd030209

Gelaro, R., McCarty, W., Suárez, M. J., Todling, R., Molod, A., Takacs, L., . . . Zhao, B. (2017). The Modern-Era Retrospective Analysis for Research and Applications, Version 2 (MERRA-2). *Journal of Climate, 30*(14), 5419-5454. doi:10.1175/jcli-d-16-0758.1

Ginoux, P., Prospero, J. M., Gill, T. E., Hsu, N. C., & Zhao, M. (2012). Global-scale attribution of anthropogenic and natural dust sources and their emission rates based on MODIS Deep Blue aerosol products. *Rev. Geophys., 50*(3), RG3005. doi:10.1029/2012rg000388

Gläser, G., Wernli, H., Kerkweg, A., & Teubler, F. (2015a). The transatlantic dust transport from North Africa to the Americas—Its characteristics and source regions. *Journal of Geophysical Research: Atmospheres, 120*(21), 11,231-211,252. doi:10.1002/2015jd023792

Gläser, G., Wernli, H., Kerkweg, A., & Teubler, F. (2015b). The transatlantic dust transport from North Africa to the Americas—Its characteristics and source regions. *Journal of Geophysical Research: Atmospheres, 120*(21), 2015JD023792. doi:10.1002/2015JD023792

Groß, S., Freudenthaler, V., Schepanski, K., Toledano, C., Schäfler, A., Ansmann, A., & Weinzierl, B. (2015). Optical properties of long-range transported Saharan dust over Barbados as measured by dual-wavelength depolarization Raman lidar measurements. *Atmospheric Chemistry and Physics*(19), 11067-11080. doi:10.5194/acp-15-11067-2015

Herbert, R. J., Krom, M. D., Carslaw, K. S., Stockdale, A., Mortimer, R. J. G., Benning, L. G., . . . Browse, J. (2018). The Effect of Atmospheric Acid Processing on the Global Deposition of Bioavailable Phosphorus From Dust. *Global Biogeochemical Cycles, 32*(9), 1367-1385. doi:doi:10.1029/2018GB005880

Hernández, O. J. R. (2014). Intrusiones de polvo africano en la región Caribe de Colombia. *Gestión y Ambiente, 17*(2), 11-29.

Hoelzemann, J. J., Longo, K. M., Fonseca, R. M., do Rosário, N. M. E., Elbern, H., Freitas, S. R., & Pires, C. (2009). Regional representativity of AERONET observation sites during the biomass burning season in South America determined by correlation studies with MODIS Aerosol Optical Depth. *Journal of Geophysical Research: Atmospheres, 114*(D13). doi:10.1029/2008jd010369

Hsu, N. C., Gautam, R., Sayer, A. M., Bettenhausen, C., Li, C., Jeong, M. J., . . . Holben, B. N. (2012). Global and regional trends of aerosol optical depth over land and ocean using SeaWiFS measurements from 1997 to 2010. *Atmos. Chem. Phys., 12*(17), 8037-8053. doi:10.5194/acp-12-8037-2012

Huang, J., Chidong, Z., & Prospero, J. M. (2010). African dust outbreaks: A satellite perspective of temporal and spatial variability over the tropical Atlantic Ocean. *Journal of Geophysical Research D: Atmospheres, 115*(5). doi:10.1029/2009jd012516

Huang, J., Zhang, C., & Prospero, J. M. (2010). African dust outbreaks: A satellite perspective of temporal and spatial variability over the tropical Atlantic Ocean. *Journal of Geophysical Research: Atmospheres, 115*(D5), D05202. doi:10.1029/2009JD012516

Ito, A., Myriokefalitakis, S., Kanakidou, M., Mahowald, N. M., Scanza, R. A., Hamilton, D. S., . . . Duce, R. A. (2019). Pyrogenic iron: The missing link to high iron solubility in aerosols. *Science Advances, 5*(5), eaau7671. doi:10.1126/sciadv.aau7671

Johnson, M., Meskhidze, N., Kiliyanpilakkil, V., & Gassó, S. (2011). Understanding the transport of Patagonian dust and its influence on marine biological activity in the South Atlantic Ocean. *Atmospheric Chemistry & Physics, 11*(6). doi:10.5194/acp-11-2487-2011

©2020 American Geophysical Union. All rights reserved.

Karyampudi, V. M., Palm, S. P., Reagen, J. A., Fang, H., Grant, W. B., Hoff, R. M., . . . Browell, E. V. (1999). Validation of the Saharan dust plume conceptual model using lidar, Meteosat, and ECMWF data. *Bulletin of the American Meteorological Society, 80*(6), 1045-1076.

Kaufman, Y., Koren, I., Remer, L., Tanré, D., Ginoux, P., & Fan, S. (2005). Dust transport and deposition observed from the Terra-Moderate Resolution Imaging Spectroradiometer (MODIS) spacecraft over the Atlantic Ocean. *Journal of Geophysical Research: Atmospheres, 110*(D10).

Kienast, S., Winckler, G., Lippold, J., Albani, S., & Mahowald, N. (2016). Tracing dust input to the global ocean using thorium isotopes in marine sediments: ThoroMap. *Global Biogeochemical Cycles, 30*(10), 1526-1541.

Kohfeld, K. E., & Harrison, S. P. (2001). DIRTMAP: the geological record of dust. *Earth-Science Reviews, 54*(1-3), 81-114.

Koren, I., Kaufman, Y. J., Washington, R., Todd, M. C., Rudich, Y., Martins, J. V., & Rosenfeld, D. (2006). The Bodele depression: a single spot in the Sahara that provides most of the mineral dust to the Amazon forest. *Environmental Research Letters, 1*(1). doi:014005

Kumar, A., Abouchami, W., Galer, S. J. G., Singh, S. P., Fomba, K. W., Prospero, J. M., & Andreae, M. O. (2018). Seasonal radiogenic isotopic variability of the African dust outflow to the tropical Atlantic Ocean and across to the Caribbean. *Earth and Planetary Science Letters, 487*, 94-105. doi:https://doi.org/10.1016/j.epsl.2018.01.025

Li, F., Ginoux, P., & Ramaswamy, V. (2010). Transport of Patagonian dust to Antarctica. *Journal of Geophysical Research: Atmospheres, 115*(D18).

Mahowald, N., Jickells, T. D., Baker, A. R., Artaxo, P., Benitez-Nelson, C. R., Bergametti, G., . . . Tsukuda, S. (2008). Global distribution of atmospheric phosphorus sources, concentrations and deposition rates, and anthropogenic impacts. *Global Biogeochemical Cycles, 22*(4). doi:doi:10.1029/2008GB003240

Mahowald, N. M., Artaxo, P., Baker, A. R., Jickells, T. D., Okin, G. S., Randerson, J. T., & Townsend, A. R. J. G. B. C. (2005). Impacts of biomass burning emissions and land use change on Amazonian atmospheric phosphorus cycling and deposition. *19*(4).

Malavelle, F. F., Haywood, J. M., Mercado, L. M., Folberth, G. A., Bellouin, N., Sitch, S., & Artaxo, P. (2019). Studying the impact of biomass burning aerosol radiative and climate effects on the Amazon rainforest productivity with an Earth system model. *Atmospheric Chemistry and Physics, 19*, 1301-1326.

Martin, S. T., Andreae, M. O., Artaxo, P., Baumgardner, D., Chen, Q., Goldstein, A. H., . . . Trebs, I. (2010). Sources and properties of Amazonian aerosol particles. *Reviews of Geophysics, 48*(2). doi:10.1029/2008RG000280

Mehta, M., Singh, R., Singh, A., Singh, N., & Anshumali. (2016). Recent global aerosol optical depth variations and trends — A comparative study using MODIS and MISR level 3 datasets. *Remote Sensing of Environment, 181*, 137-150. doi:https://doi.org/10.1016/j.rse.2016.04.004

Mercado, L. M., Patiño, S., Domingues, T. F., Fyllas, N. M., Weedon, G. P., Sitch, S., . . . Lloyd, J. (2011). Variations in Amazon forest productivity correlated with foliar nutrients and modelled rates of photosynthetic carbon supply. *Philosophical Transactions of the Royal Society B: Biological Sciences, 366*(1582), 3316-3329. doi:doi:10.1098/rstb.2011.0045

Mok, J., Krotkov, N. A., Arola, A., Torres, O., Jethva, H., Andrade, M., . . . Ren, X. (2016). Impacts of brown carbon from biomass burning on surface UV and ozone photochemistry in the Amazon Basin. *Scientific Reports, 6*, 36940. doi:10.1038/srep36940 https://www.nature.com/articles/srep36940#supplementary-information

Moran-Zuloaga, D., Ditas, F., Walter, D., Saturno, J., Brito, J., Carbone, S., . . . Pöhlker, C. (2018). Long-term study on coarse mode aerosols in the Amazon rain forest with the frequent intrusion of Saharan dust plumes. *Atmos. Chem. Phys., 18*(13), 10055-10088. doi:10.5194/acp-18-10055-2018

Myriokefalitakis, S., Nenes, A., Baker, A. R., Mihalopoulos, N., & Kanakidou, M. (2016). Bioavailable atmospheric phosphorous supply to the global ocean: a 3-D global modeling study. *Biogeosciences, 13*(24), 6519-6543. doi:10.5194/bg-13-6519-2016

Nicholson, S. E. (2015). Evolution and current state of our understanding of the role played in the climate system by land surface processes in semi-arid regions. *Global and Planetary Change, 133*, 201-222. doi:http://dx.doi.org/10.1016/j.gloplacha.2015.08.010

Okin, G. S., Mahowald, N., Chadwick, O. A., & Artaxo, P. (2004). Impact of desert dust on the biogeochemistry of phosphorus in terrestrial ecosystems. *Global Biogeochemical Cycles, 18*(2). doi:doi:10.1029/2003GB002145

Omar, A. H., Winker, D. M., Vaughan, M. A., Hu, Y., Trepte, C. R., Ferrare, R. A., . . . Rogers, R. R. (2009). The CALIPSO automated aerosol classification and lidar ratio selection algorithm. Journal of Atmospheric and Oceanic Technology, 26(10), 1994-2014. doi:10.1175/2009JTECHA1231.1

©2020 American Geophysical Union. All rights reserved.

Pan, Y., Birdsey, R. A., Fang, J., Houghton, R., Kauppi, P. E., Kurz, W. A., . . . Hayes, D. (2011). A Large and Persistent Carbon Sink in the World's Forests. *Science, 333*(6045), 988-993. doi:10.1126/science.1201609

Pereira, G., Siqueira, R., Rosário, N. E., Longo, K. L., Freitas, S. R., Cardozo, F. S., . . . Wooster, M. J. (2016). Assessment of fire emission inventories during the South American Biomass Burning Analysis (SAMBBA) experiment. *Atmospheric Chemistry and Physics, 16*(11), 6961. doi:10.5194/acp-16-6961-2016

Pöhlker, C., Walter, D., Paulsen, H., Könemann, T., Rodríguez-Caballero, E., Moran-Zuloaga, D., . . . Andreae, M. O. (2019). Land cover and its transformation in the backward trajectory footprint region of the Amazon Tall Tower Observatory. *Atmos. Chem. Phys., 19*(13), 8425-8470. doi:10.5194/acp-19-8425-2019

Pöhlker, M. L., Ditas, F., Saturno, J., Klimach, T., Hrabě de Angelis, I., Araùjo, A. C., . . . Chi, X. (2018). Long-term observations of cloud condensation nuclei over the Amazon rain forest–Part 2: Variability and characteristics of biomass burning, long-range transport, and pristine rain forest aerosols. *Atmospheric Chemistry and Physics, 18*(14), 10289-10331.

Pöhlker, M. L., Pöhlker, C., Ditas, F., Klimach, T., Hrabe de Angelis, I., Araújo, A., . . . Pöschl, U. (2016). Long-term observations of cloud condensation nuclei in the Amazon rain forest – Part 1: Aerosol size distribution, hygroscopicity, and new model parametrizations for CCN prediction. *Atmos. Chem. Phys., 16*(24), 15709-15740. doi:10.5194/acp-16-15709-2016

Pourmand, A., Prospero, J. M., & Sharifi, A. (2014). Geochemical fingerprinting of trans-Atlantic African dust based on radiogenic Sr-Nd-Hf isotopes and rare earth element anomalies. *Geology*. doi:10.1130/g35624.1

Prospero, J. (1968). Atmospheric dust studies on Barbados. *Bulletin of the American Meteorological Society, 49*(6), 645-652.

Prospero, J., Glaccum, R., & Nees, R. (1981). Atmospheric transport of soil dust from Africa to South America. *Nature, 289*(5798), 570-572.

Prospero, J. M. (2002). The chemical and physical properties of marine aerosols: An introduction. *Chemistry of Marine Water and Sediments*, 35–82.

Prospero, J. M. (2015). Characterizing the temporal and spatial variability of African dust over the Atlantic. *DUST, 24*, 68.

Prospero, J. M., Bonatti, E., Schubert, C., & Carlson, T. N. (1970). Dust in the Caribbean atmosphere traced to an African dust storm. *Earth and Planetary Science Letters, 9*(3), 287-293.

Prospero, J. M., & Carlson, T. N. (1972). Vertical and Areal Distribution of Saharan Dust over the Western Equatorial North Atlantic Ocean. *J. Geophys. Res., 77*(27), 5255-5265. doi:doi:10.1029/JC077i027p05255

Prospero, J. M., Collard, F. X., Molinié, J., & Jeannot, A. (2014). Characterizing the annual cycle of African dust transport to the Caribbean Basin and South America and its impact on the environment and air quality. *Global Biogeochemical Cycles, 28*(7), 757-773.

Prospero, J. M., Ginoux, P., Torres, O., Nicholson, S. E., & Gill, T. E. (2002). Environmental characterization of global sources of atmospheric soil dust identified with the NIMBUS 7 Total Ozone Mapping Spectrometer (TOMS) absorbing aerosol product. *Rev. Geophys., 40*(1), 1002. doi:10.1029/2000rg000095

Prospero, J. M., & Lamb, P. J. (2003). African Droughts and Dust Transport to the Caribbean: Climate Change Implications. *Science, 302*(5647), 1024-1027. doi:10.1126/science.1089915

Prospero, J. M., Landing, W. M., & Schulz, M. (2010). African dust deposition to Florida: Temporal and spatial variability and comparisons to models. *J. Geophys. Res., 115*(D13), D13304. doi:10.1029/2009jd012773

Prospero, J. M., & Mayol-Bracero, O. L. (2013). Understanding the transport and impact of African dust on the Caribbean Basin. *Bulletin of the American Meteorological Society, 94*(9), 1329-1337. doi:10.1175/BAMS-D-12-00142.1

Prospero, J. M., & Nees, R. T. (1977). Dust concentration in the atmosphere of the equatorial North Atlantic: Possible relationship to the Sahelian drought. *Science, 196*(4295), 1196-1198.

Prospero, J. M., Olmez, I., & Ames, M. (2001). Al and Fe in PM 2.5 and PM 10 suspended particles in South-Central Florida: The impact of the long range transport of African mineral dust. *Water, Air, and Soil Pollution, 125*(1-4), 291-317. doi:10.1023/a:1005277214288

Querol, X., Tobías, A., Pérez, N., Karanasiou, A., Amato, F., Stafoggia, M., . . . Alastuey, A. (2019). Monitoring the impact of desert dust outbreaks for air quality for health studies. *Environment International, 130*, 104867. doi:https://doi.org/10.1016/j.envint.2019.05.061

Randles, C. A. (2016). *Technical Report Series on Global Modeling and Data Assimilation*. Retrieved from

©2020 American Geophysical Union. All rights reserved.

Randles, C. A., Silva, A. M. d., Buchard, V., Colarco, P. R., Darmenov, A., Govindaraju, R., . . . Flynn, C. J. (2017). The MERRA-2 Aerosol Reanalysis, 1980 Onward. Part I: System Description and Data Assimilation Evaluation. *Journal of Climate, 30*(17), 6823-6850. doi:10.1175/jcli-d-16-0609.1

Ridley, A. D., Heald, L. C., Kok, F. J., & Zhao, C. (2016). An observationally constrained estimate of global dust aerosol optical depth. *Atmospheric Chemistry and Physics, 16*(23), 15097-15117. doi:10.5194/acp-16-15097-2016

Ridley, D. A., Heald, C., L., & Ford, B. (2012). North African dust export and deposition: A satellite and model perspective. *Journal of Geophysical Research: Atmospheres, 117*(D2).

Ridley, D. A., Heald, C. L., Kok, J. F., & Zhao, C. (2016). An observationally constrained estimate of global dust aerosol optical depth. *Atmospheric Chemistry and Physics, 16*(23), 15097-15117. doi:10.5194/acp-16-15097-2016

Rittmeister, F., Ansmann, A., Engelmann, R., Skupin, A., Baars, H., Kanitz, T., & Kinne, S. (2017). Profiling of Saharan dust from the Caribbean to western Africa-Part 1: Layering structures and optical properties from shipborne polarization/Raman lidar observations. *Atmospheric Chemistry and Physics, 17*(21), 12963-12983. doi:10.5194/acp-17-12963-2017

Rizzolo, J. A., Barbosa, C. G. G., Borillo, G. C., Godoi, A. F. L., Souza, R. A. F., Andreoli, R. V., . . . Godoi, R. H. M. (2017). Soluble iron nutrients in Saharan dust over the central Amazon rainforest. *Atmospheric Chemistry and Physics, 17*(4), 2673-2687. doi:10.5194/acp-17-2673-2017

Romero, O. E., Lange, C. B., Swap, R., & Wefer, G. (1999). Eolian-transported freshwater diatoms and phytoliths across the equatorial Atlantic record: Temporal changes in Saharan dust transport patterns. *Journal of Geophysical Research: Oceans, 104*(C2), 3211-3222. doi:10.1029/1998JC900070

Rudnick, R. L., & Gao, S. (2003). Composition of the continental crust. In *Treatise on geochemistry* (Vol. 3, pp. 659).

Saturno, J., Holanda, B. A., Pöhlker, C., Ditas, F., Wang, Q., Moran-Zuloaga, D., . . . Andreae, M. O. (2018). Black and brown carbon over central Amazonia: Long-term aerosol measurements at the ATTO site. *Atmospheric Chemistry and Physics, 18*(17), 12817-12843. doi:10.5194/acp-18-12817-2018

Savoie, D. L., Arimoto, R., Keene, W. C., Prospero, J. M., Duce, R. A., & Galloway, J. N. (2002). Marine biogenic and anthropogenic contributions to non-sea-salt sulfate in the marine boundary layer over the North Atlantic Ocean. *J. Geophys. Res., 107*(D18), 4356. doi:10.1029/2001jd000970

Savoie, D. L., Prospero, J. M., & Saltzman, E. S. (1989). Non-sea-salt sulfate and nitrate in trade wind aerosols at Barbados: Evidence for long-range transport. *Journal of Geophysical Research: Atmospheres, 94*(D4), 5069-5080.

Schepanski, K., Heinold, B., & Tegen, I. (2017). Harmattan, Saharan heat low, and West African monsoon circulation: modulations on the Saharan dust outflow towards the North Atlantic. *Atmos. Chem. Phys., 17*(17), 10223-10243. doi:10.5194/acp-17-10223-2017

Sheen, K. L., Smith, D. M., Dunstone, N. J., Eade, R., Rowell, D. P., & Vellinga, M. (2017). Skilful prediction of Sahel summer rainfall on inter-annual and multi-year timescales. *Nature Communications, 8*, 14966. doi:10.1038/ncomms14966
https://www.nature.com/articles/ncomms14966#supplementary-information

Shikwambana, L., & Sivakumar, V. (2018). Global distribution of aerosol optical depth in 2015 using CALIPSO level 3 data. *Journal of Atmospheric and Solar-Terrestrial Physics, 173*, 150-159. doi:https://doi.org/10.1016/j.jastp.2018.04.003

Stong, C. L. (1961). The Amateur Scientist: An amateur investigates the origin of Venezuela's peculiar fog: the calina. *Scientific American, 205*(October), 172 - 183.

Swap, R., Garstang, M., Greco, S., Talbot, R., & Kållberg, P. (1992). Saharan dust in the Amazon Basin. *Tellus B: Chemical and Physical Meteorology, 44*(2), 133-149. doi:10.3402/tellusb.v44i2.15434

Tipping, E., Benham, S., Boyle, J. F., Crow, P., Davies, J., Fischer, U., . . . Toberman, H. (2014). Atmospheric deposition of phosphorus to land and freshwater. *Environmental Science: Processes & Impacts, 16*(7), 1608-1617. doi:10.1039/C3EM00641G

Trapp, J. M., Millero, F. J., & Prospero, J. M. (2010). Temporal variability of the elemental composition of African dust measured in trade wind aerosols at Barbados and Miami. *Marine Chemistry, 120*(1-4), 71-82. Retrieved from http://www.scopus.com/inward/record.url?eid=2-s2.0-74049122665&partnerID=40&md5=7b78914da6c8f2299e1d5d6497a02d24

Tsamalis, C., Chédin, A., Pelon, J., & Capelle, V. (2013). The seasonal vertical distribution of the saharan air layer and its modulation by the wind. *Atmospheric Chemistry and Physics, 13*(22), 11235-11257. doi:10.5194/acp-13-11235-2013

Vet, R., Artz, R. S., Carou, S., Shaw, M., Ro, C.-U., Aas, W., . . . Galy-Lacaux, C. (2014). A global assessment of precipitation chemistry and deposition of sulfur, nitrogen, sea salt, base cations, organic acids, acidity and pH, and phosphorus. *Atmospheric Environment, 93*, 3-100.

©2020 American Geophysical Union. All rights reserved.

Warren, A., Chappell, A., Todd, M. C., Bristow, C., Drake, N., Engelstaedter, S., . . . Washington, R. (2007). Dust-raising in the dustiest place on earth. *Geomorphology, 92*(1-2), 25-37. doi:10.1016/j.geomorph.2007.02.007

Weinzierl, B., Ansmann, A., Prospero, J. M., Althausen, D., Benker, N., Chouza, F., . . . Walser, A. (2017). The Saharan Aerosol Long-Range Transport and Aerosol–Cloud-Interaction Experiment: Overview and Selected Highlights. *Bulletin of the American Meteorological Society, 98*(7), 1427-1451. doi:10.1175/bams-d-15-00142.1

Winker, D., Pelon, J., Coakley Jr, J., Ackerman, S., Charlson, R., Colarco, P., . . . Kittaka, C. (2010). The CALIPSO mission: A global 3D view of aerosols and clouds. *Bulletin of the American Meteorological Society, 91*(9), 1211-1230.

Yu, H., Chin, M., Bian, H., Yuan, T., Prospero, J. M., Omar, A. H., . . . Zhang, Z. (2015). Quantification of trans-Atlantic dust transport from seven-year (2007–2013) record of CALIPSO lidar measurements. *Remote Sensing of Environment, 159*, 232-249. doi:https://doi.org/10.1016/j.rse.2014.12.010

Yu, H., Chin, M., Yuan, T., Bian, H., Remer, L. A., Prospero, J. M., . . . Zhao, C. (2015). The fertilizing role of African dust in the Amazon rainforest: A first multiyear assessment based on data from Cloud-Aerosol Lidar and Infrared Pathfinder Satellite Observations. *Geophysical Research Letters, 42*(6), 1984-1991. doi:10.1002/2015GL063040

Yu, H., Remer, L. A., Kahn, R. A., Chin, M., & Zhang, Y. (2013). Satellite perspective of aerosol intercontinental transport: From qualitative tracking to quantitative characterization. *Atmospheric Research, 124*, 73-100. doi:https://doi.org/10.1016/j.atmosres.2012.12.013

Yu, H., Tan, Q., Chin, M., Remer, L. A., Kahn, R. A., Bian, H., . . . Omar, A. H. (2019). Estimates of African Dust Deposition Along the Trans-Atlantic Transit Using the Decadelong Record of Aerosol Measurements from CALIOP, MODIS, MISR, and IASI. *Journal of Geophysical Research: Atmospheres, 124*(14), 7975-7996.

Zamora, L. M., Prospero, J. M., Hansell, D. A., & Trapp, J. M. (2013). Atmospheric P deposition to the subtropical North Atlantic: sources, properties, and relationship to N deposition. *Journal of Geophysical Research: Atmospheres, 118*(3), 1546-1562. doi:10.1002/jgrd.50187

Zhang, X., Zhao, L., Tong, D., Wu, G., Dan, M., & Teng, B. (2016). A systematic review of global desert dust and associated human health effects. *Atmosphere, 7*(12), 158. doi:10.3390/atmos7120158

Zhao, W., Balsam, W., Williams, E., Long, X., & Ji, J. (2018). Sr–Nd–Hf isotopic fingerprinting of transatlantic dust derived from North Africa. *Earth and Planetary Science Letters, 486*, 23-31. doi:https://doi.org/10.1016/j.epsl.2018.01.004

Zuidema, P., Alvarez, C., Kramer, S. J., Custals, L., Izaguirre, M., Sealy, P., . . . Blades, E. (2019). Is summer African dust arriving earlier to Barbados? The updated long-term in-situ dust mass concentration time series from Ragged Point, Barbados and Miami, Florida. *Bulletin of the American Meteorological Society, 100*(10), 1981-1986 doi:10.1175/bams-d-18-0083.1

Zuloaga, G. (1966). La calina y el viento salante. *Boletín Academia de Ciencias Físicas, Matemáticas y Naturales, 26*, .101-114.

Accepted Article

©2020 American Geophysical Union. All rights reserved.

Table 1. MERRA-2 Dust Deposition to a Grid of Five Degree Boxes, 2002-2017: Units, Tg per box.^

Period	Box Corner#	Box	Box	Box	Box	Box	Box	Latitude Total	Season %
	SW	-75,5	-70,5	-65,5					
	NE	-70,10	-65,10	-60,10					
Annual		**0.67**	**0.56**	**0.82**				**2.05**	
JFMAM!		0.30	0.16	0.30				0.76	37%
MJJAS!		0.33	0.37	0.47				1.17	57%
						Cayenne			
	SW	-75,0	-70,0	-65,0	-60,0	***-55,0***			
	NE	-70,5	-65,5	-60,5	-55,5	***-50,5***			
Annual		**0.38**	**0.54**	**0.63**	**0.71**	***1.30***		**3.56**	
JFMAM!		0.17	0.25	0.32	0.45	***0.95***		2.15	60%
MJJAS!		0.18	0.25	0.27	0.22	***0.28***		1.20	34%
					ATTO				
	SW	-75,-5	-70,-5	-65,-5	***-60,-5***	-55-5	-50,-5		
	NE	-70,0	-65,0	-60,0	***-55,0***	-50,0	-45,0		
Annual		**0.29**	**0.33**	**0.39**	***0.37***	**0.41**	**0.62**	**2.41**	
JFMAM!		0.12	0.18	0.24	***0.24***	0.32	0.50	1.60	66%
MJJAS!		0.12	0.12	0.10	***0.08***	0.06	0.08	0.55	23%
Annual Total: 10°N to 5°S								**8.02**	
JFMAM: 10°N to 5°S								4.50	0.56
MJJAS: 10°N TO 5°S								2.82	0.36

^To estimate Dust-P deposition, multiply dust deposition values by $1x10^{-3}$.
!Cayenne winter-spring dust season: JFMA plus half of May. Caribbean dust season: JJAS plus half of May.
#Defines the SW and NE corners of the model box according to the MERRA-2 format on the NASA Giovanni web site https://giovanni.gsfc.nasa.gov/giovanni/).

Accepted Article

©2020 American Geophysical Union. All rights reserved.

Table 2. Estimates of Annual Dust Deposition Into the Amazon Basin and Associated Phosphorus Deposition#

Source	Dust Deposition Total Tg a^{-1}	Dust Deposition Rate kg ha^{-1} a-1	P Deposition+ Total Tg P a^{-1}	P Deposition+ Rate g P ha^{-1} a^{-1}	References
CALIOP	28	29	0.022	23	Yu et al. (2015b)
MODIS	50	n/a	0.039	n/a	Kaufman et al. (2005)
In situ observations	13	190	n/a	148	Swap et al. (1992)
GOCART model	26	27	0.020	21	Yu et al. (2015b); Chin et al., (2014)
WRF-Chem model	19	20	0.015	16	Yu et al. (2015b)
GEOS-Chem model*	17	n/a	0.013	n/a	Ridley et al. (2012)
GLOMAP/TOMCAT	32	33	0.025	26	Herbert et al. (2018)^
MATCH	n/a	n/a	n/a	20 - 50	Mahowald et al. (2005)
CAM/MATCH	n/a	n/a	0.011-0.033	11-35	Barkley et al., (2019)
ECHAM5	34.3/11.4	44/14.6	0.027/0.01	34/11	Gläser et al. (2015a)[$]
MERRA-2 model	8.0	10.5	0.0062	9.0	This paper

+Assumes P concentration 780 ppm in dust.
[#]Table extracted in part from Yu et al. (2015b).
*GEOS-Chem = Goddard Earth Observing System coupled with chemistry.
^ Assumes the same deposition area as Yu *et al.* See text.
[$] Computed by two different methods. Total annual.

Accepted Article

©2020 American Geophysical Union. All rights reserved.

Table 3. Summary of Seasonal Dust Deposition Rates to the Amazon Basin (Units: Tg dust total)

	DJF	MAM	JIA	SON	Annual Total
Yu *et al.*, 2007-2013: CALIOP*	13.3	15.0	0.0	0.0	28.3
Yu *et al.*, 2007-2013: GOCART*	8.2	10.3	..……6.6…..…		25.1
Ridley *et al.*, 2006-2008^	3.7	7.9	5.2	0.5	17.3
Glaser *et al.*, 2015: Eularian[&]	8.9	9.1	8.5	3.8	30.3
Glaser *et al.*, 2015: Lagrangian[&]	4.9	2.8	2.4	1.3	11.4
Prospero *et al.*, 2002-2017[@]	1.5	3.9	2.1	0.5	8.0

* Yu *et al.*, 2015b, Table 1
^ Ridley *et al.*, 2012, Table 3
& Glaser *et al.*, 2015, Table 1
@ This paper

Accepted Article

©2020 American Geophysical Union. All rights reserved.

Figure 1: Northern South America showing the location of Cayenne, where the research site is located. Also shown is the location of the Amazon Tall Tower Observatory (ATTO), a research site located near Manaus, Brazil (Andreae et al., 2015). The area outlined in red encompasses the five-degree-grid box array used in computing MERRA-2 monthly mean surface dust concentrations and total deposition rates. (Image from Google Earth Pro.)

Accepted Article

©2020 American Geophysical Union. All rights reserved.

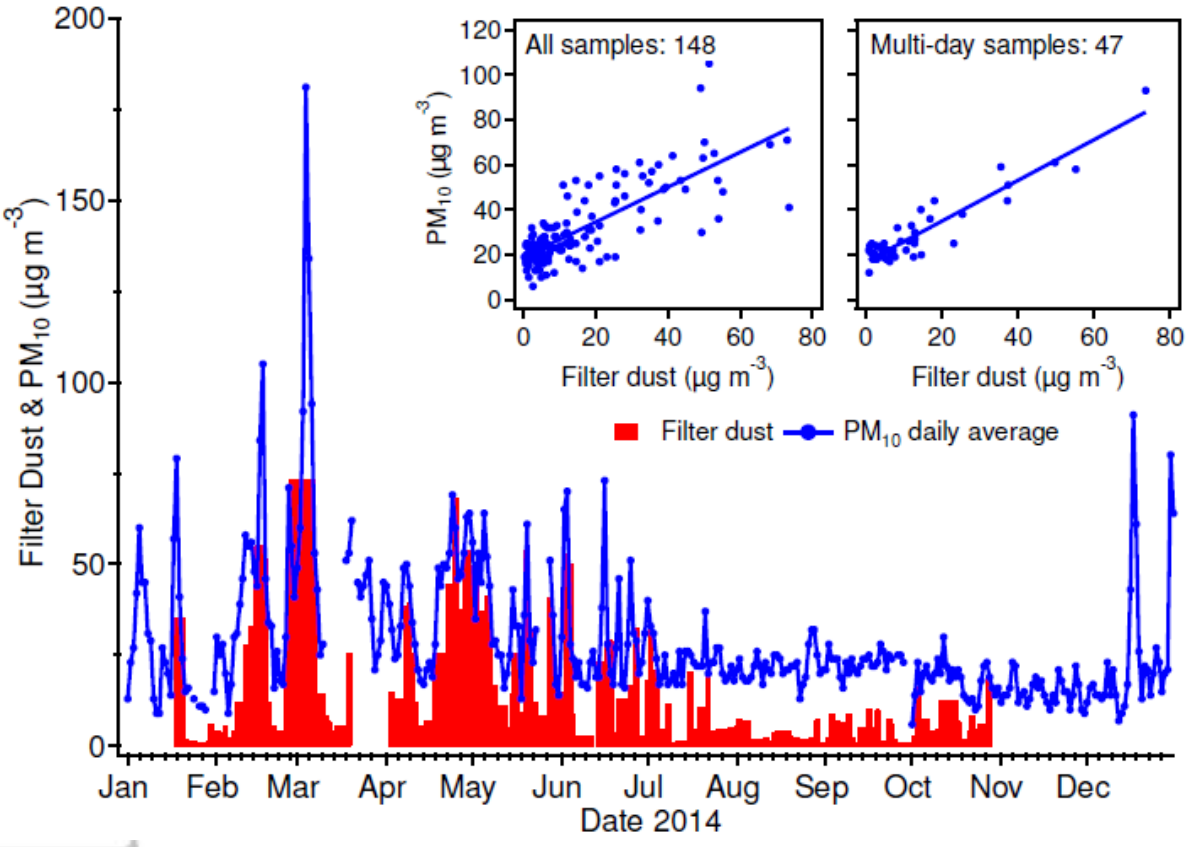

Figure 2: Cayenne daily mean PM_{10} (blue) and mineral dust concentration (red) based on filter ash residues. PM_{10} means are calculated from the daily means of all PM_{10} instruments operating on any given day. Blank spaces indicate that no sample was taken. PM_{10} daily means are calculated midnight-to-midnight, local time. Filter measurements are made over a nominal 24-hour period which typically begins around local noon. Inset, left: scatter plot of all daily average PM_{10} against filter mineral dust atmospheric concentrations. In the case where filters were collected over two or more days, the average PM_{10} concentration for that period is used. A total of 148 samples yields $Y = 0.776x + 18.8$, the coefficient of determination, R^2, = 0.612. Inset, right: scatter plot of PM_{10} concentrations using only multi-day filter samples, a total of 47, $Y = 0.904x + 16.89$, $R^2 = 0.873$.

Accepted

©2020 American Geophysical Union. All rights reserved.

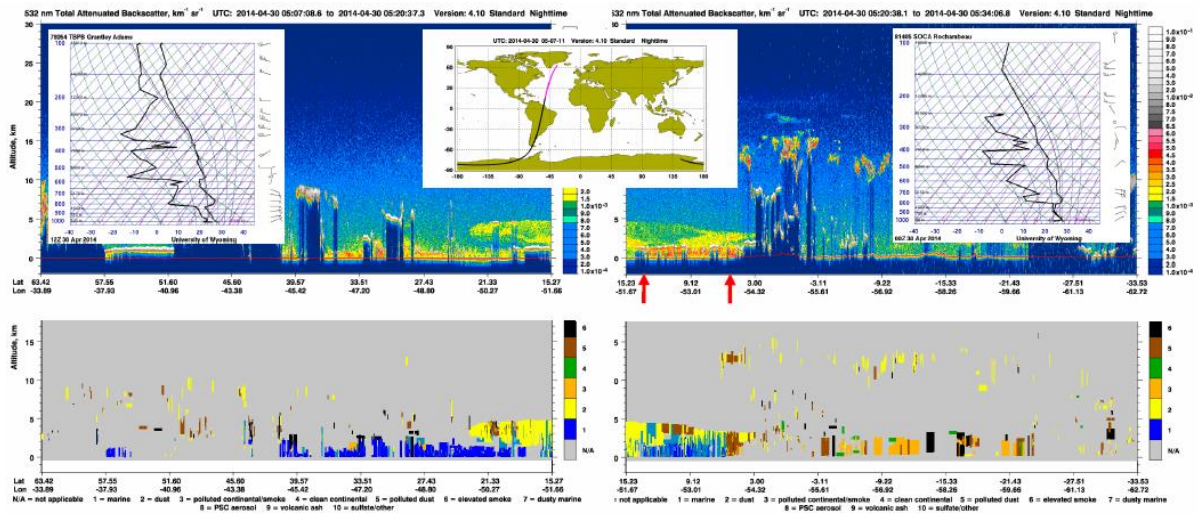

Figure 3. CALIOP aerosol vertical profile along a track that passes over Cayenne and South America (right panels) and Barbados and the western Tropical Atlantic (left panels) during a major dust event on 30 April 2014. The inset map, top center, shows the CALIOP track for the left panels in pink and the right panels in black. The upper panels show the total attenuated backscatter from all aerosols. The bottom panels show the aerosol subtype as determined by the CALIOP model algorithm (Omar et al., 2009); see the color coding scale on the lower right. Aerosol identified as "mineral dust" is shown in yellow, "polluted dust" in brown, and "marine" in blue. The red arrows at the bottom of the top right panel mark the approximate latitudes of Cayenne (04.948, -52.309) and Barbados (13.165, -59.432) along the track. Dust extends from the ITCZ at about 3°N to about 23°N. The inset sonde skew-T profiles were obtained on the same day as the CALIOP overpass at the local meteorological stations on Barbados (Grantley-Adams) and Cayenne (Rochambeau). The Saharan Air Layer (SAL) is clearly recognized in the sondes by the sharp inversion at about 2000 m at Barbados and Cayenne. The SAL top is at about 3200m at Cayenne and 4500 m at Barbados, as seen also in the CALIOP profile. (CALIOP images: https://www-calipso.larc.nasa.gov/products/lidar/browse_images/. Soundings: U. Wyoming Dept. Atmospheric Science web site: http://weather.uwyo.edu/upperair/sounding.html.)

Accepted Article

©2020 American Geophysical Union. All rights reserved.

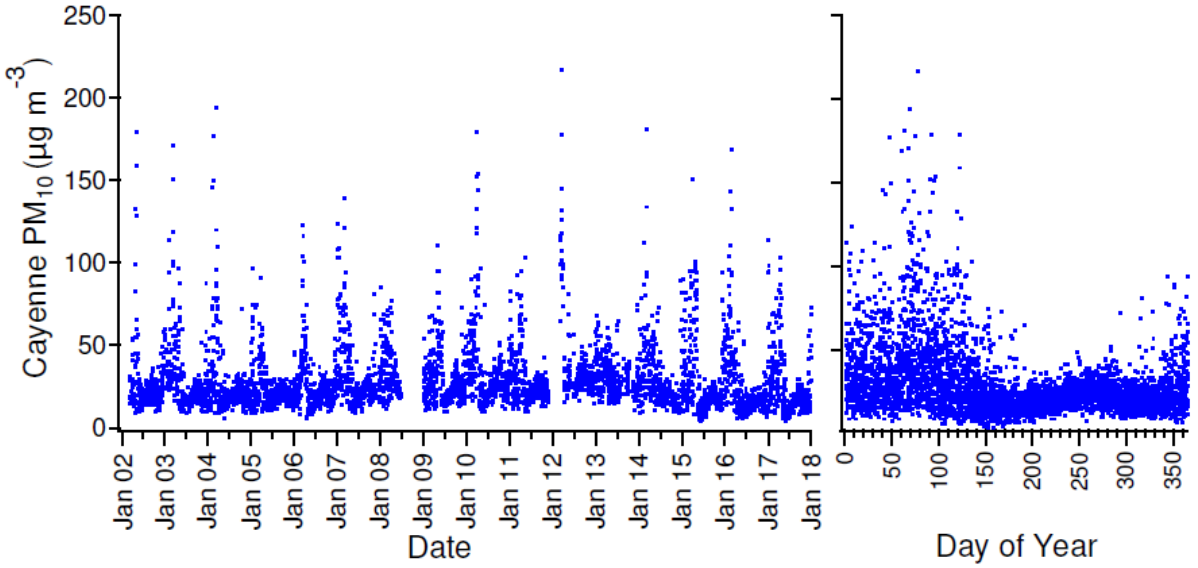

Figure 4: Cayenne daily mean PM_{10}, 2002 – 2017. Means are calculated from measurements made at all operational sites on any given day. Left: data plotted against the date. Right: against day-of-the-year. In the aggregate, transport begins in December, peaks in March and April, and abruptly ends around days 140-150 (late May). After day 150, values fall in a narrow band which steadily increases to a broad peak at about day 260-280 (September-October). Beyond day 280, PM_{10} abruptly decreases to a band of low values which continues until the start of the next dust season in early December.

Accepted Article

©2020 American Geophysical Union. All rights reserved.

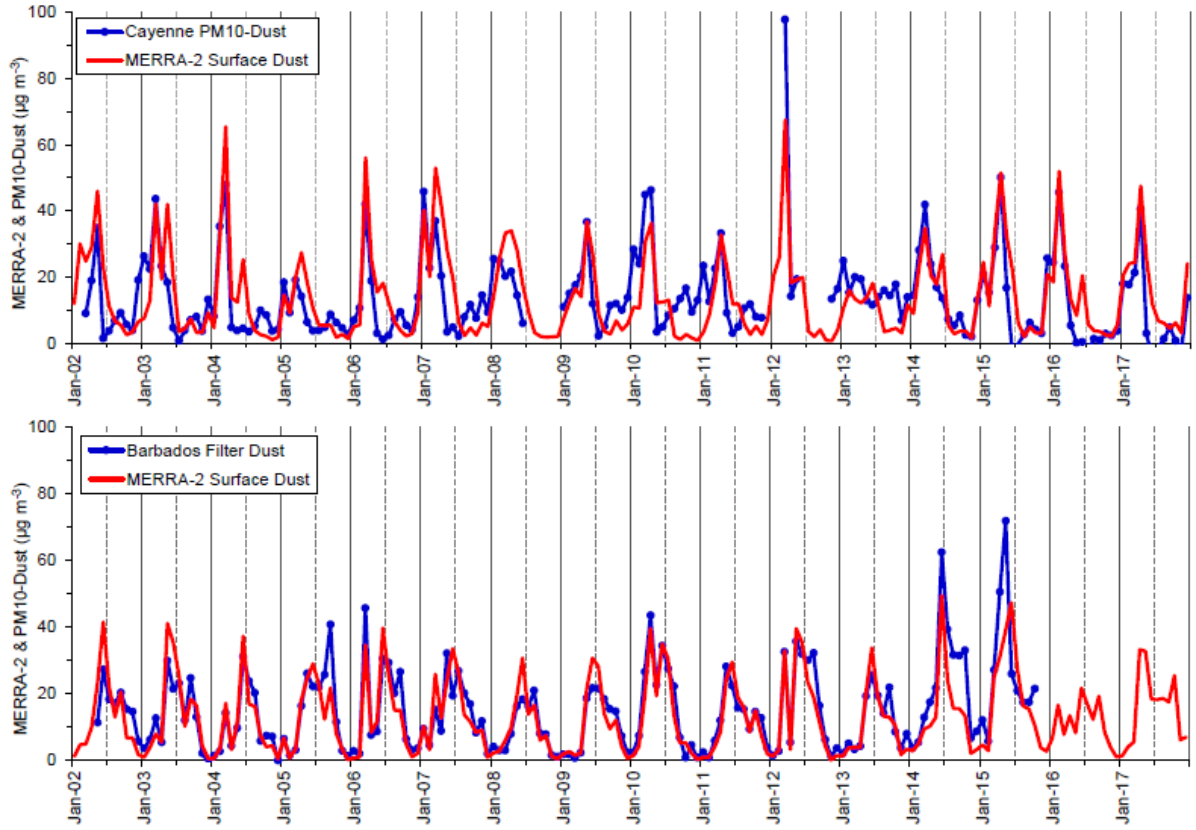

Figure 5: MERRA-2 estimates of monthly mean surface dust concentration for Cayenne (top) and Barbados (bottom) plotted with the corresponding measured dust concentrations. The MERRA-2 concentrations are computed for a 1-by-1 degree box centered on, respectively, the city of Cayenne and on Ragged Point, Barbados (Fig. 1), the site used in previous African dust studies, e.g., (Prospero & Lamb, 2003; Prospero & Mayol-Bracero, 2013; Zuidema et al., 2019).

Accepted

©2020 American Geophysical Union. All rights reserved.

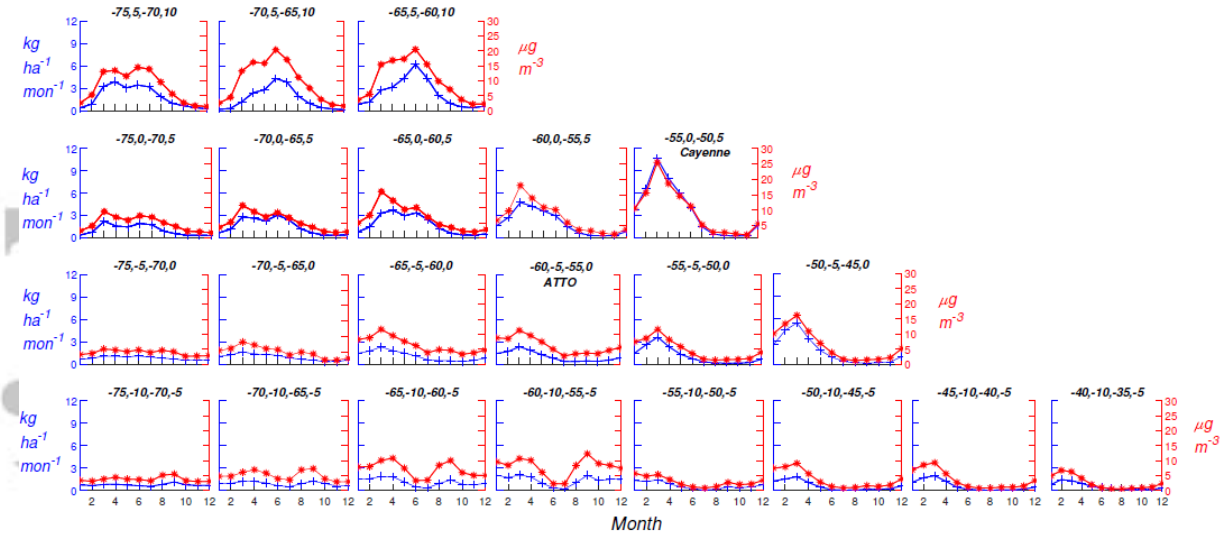

Figure 6: Monthly average MERRA-2 surface dust mass concentration (red: right axis, μg m^{-3}) and MERRA-2 wet-plus-dry dust deposition (blue: left axis, kg ha^{-1} mon^{-1}), 2002 – 2017. Model results were obtained for a grid of five-degree boxes, configured as in Fig. 1. The coordinates of the corners of each box are coded according to the format used on the NASA GIOVANNI web site: Lower left of the box: West, South; Upper right of the box: East, North. The boxes in which Cayenne and the Amazon Tall Tower Observatory (ATTO) are located are so labeled. Note that the values in the lowest tier of boxes (5°S to 10°S) are questionable for reasons discussed in the text.

Accepted Article

©2020 American Geophysical Union. All rights reserved.

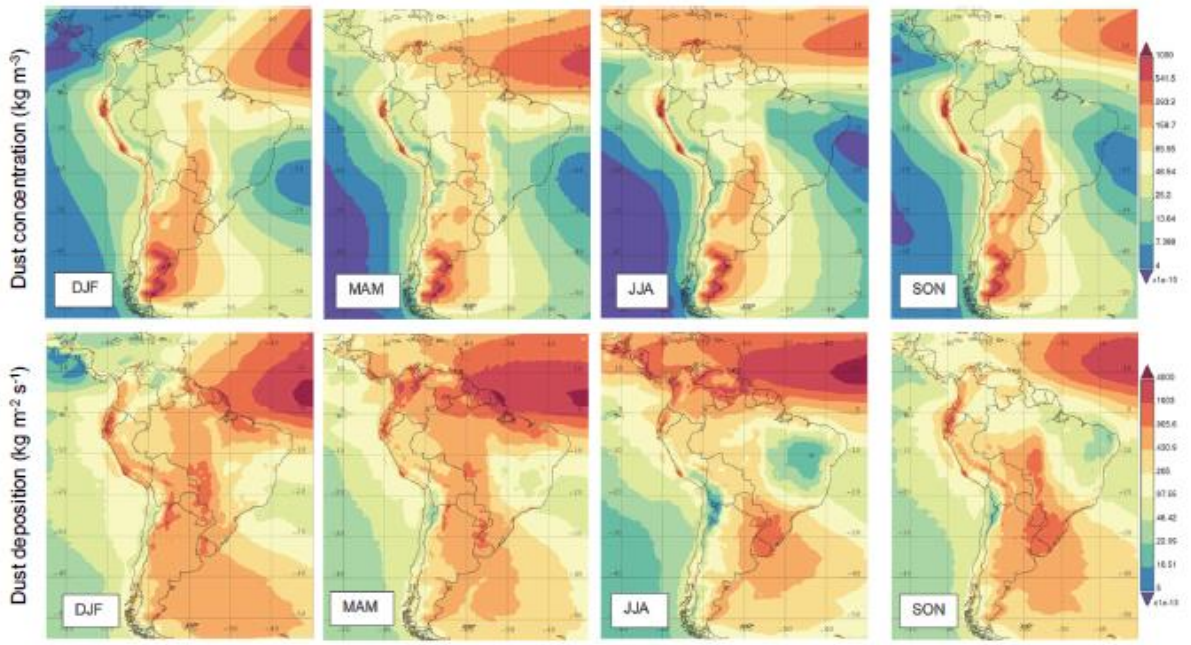

Figure 7: MERRA-2 Seasonal average surface dust concentration 2002 – 2017 (top row) and average wet-plus-dry dust deposition 2002 – 2017 (bottom row). Dust concentration: kg m^{-3} (color scale at right, top row). Dust deposition units: kg m^{-2} s^{-1} (scale at right, bottom row). The color bar scales apply to all the seasonal products in their respective rows.

Accepted

©2020 American Geophysical Union. All rights reserved.

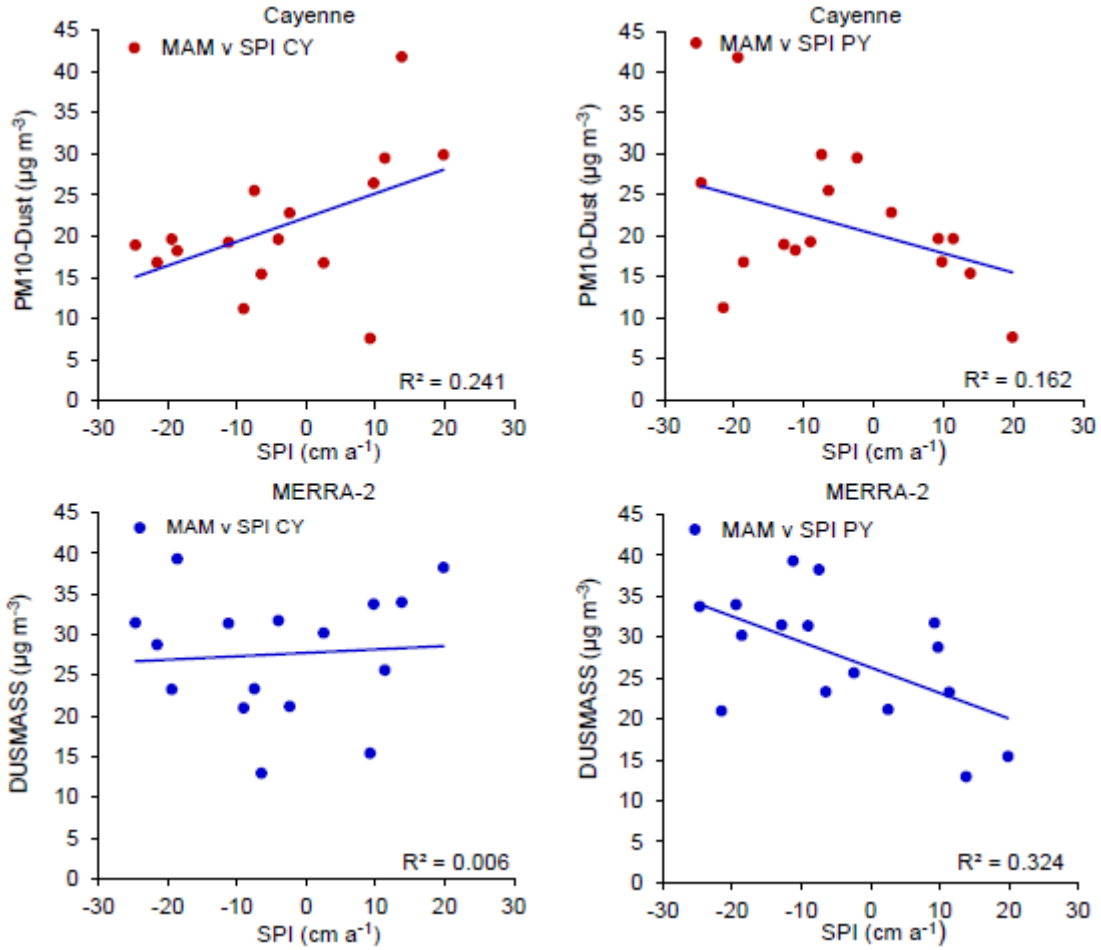

Figure 8: Cayenne PM10-Dust and Sahel Precipitation Index. 2002 – 2017. The index is the precipitation anomaly in centimeters per year with respect to the mean 1980-2009. Top plots, Cayenne MAM PM10-Dust against Current Year SPI (Fig. 8a.) and Prior Year SPI (Fig. 8b.). Bottom plots: MERRA-2 MAM Surface Dust against Current Year SPI (Fig. 8c.) and Prior Year SPI (Fig. 8d.) (SPI: http://research.jisao.washington.edu/data/sahel/)

Accepted Article

©2020 American Geophysical Union. All rights reserved.